

**Fundamental Surface Science and
Engineering Issue for High Gradient X-
band Structures at KEK**

XB0-WS

03 December 2008

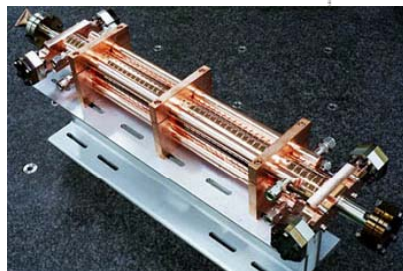
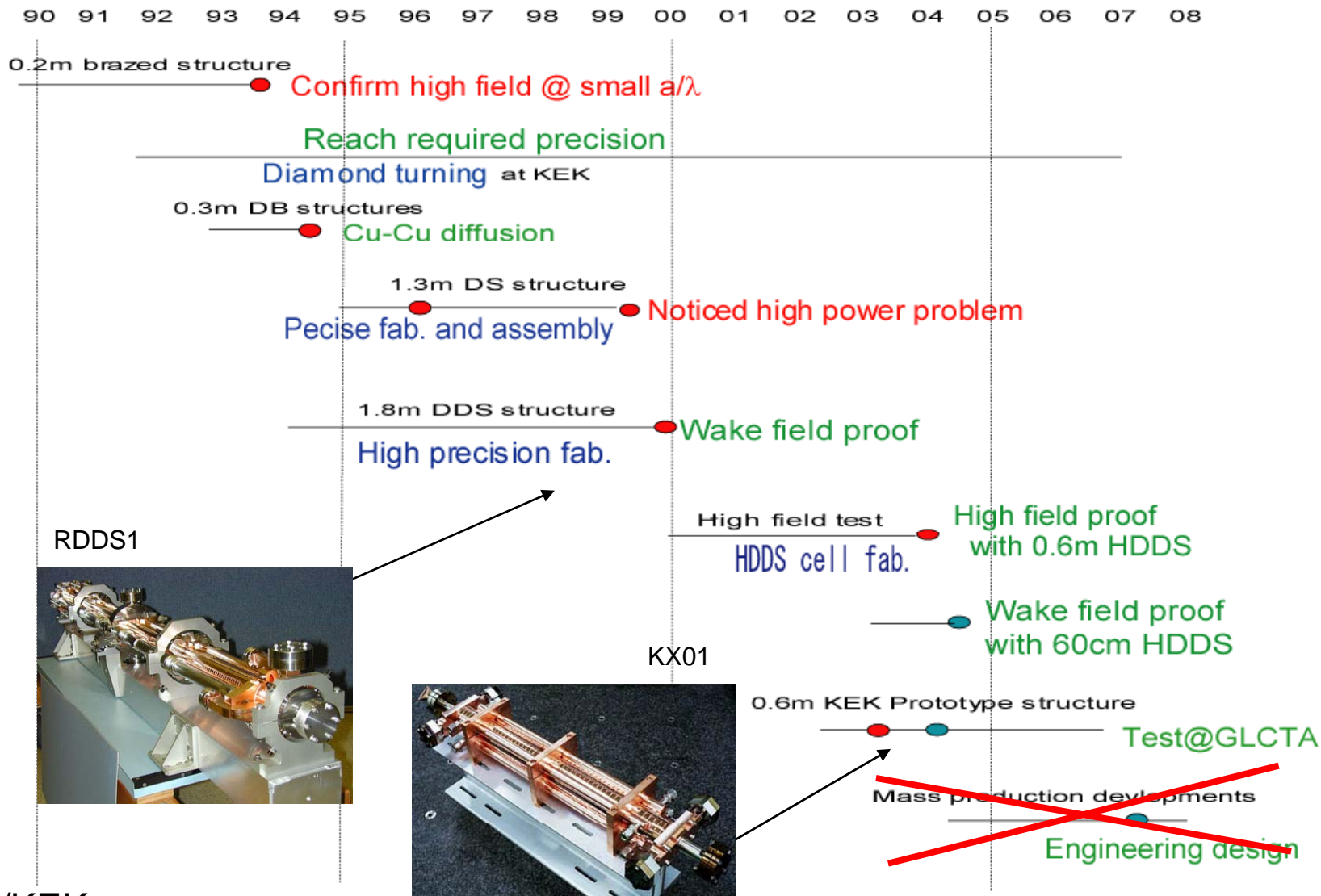
KEK

Y.Higashi

Abstract

- Since 1990 KEK has been studying X-band accelerating structure fabrication technologies and been **strongly collaborating with SLAC**. So far high gradient and weak field performance test were carried out with both laboratories.
- Currently various material, surface preparation and assemble technologies are studying **in order to understand what determine breakdown and pulse heating damage**. Especially microscopic study on materials and surface preparation are experimentally considering.
- After realization of high gradient accelerating structure, order of a few ten thousands structure sections must be manufactured with **cost performance for construction of TeV energy region accelerator**. In this presentation I will present a summary of the high gradient structure fabrication efforts at KEK and future perspective of accelerating disks/quadrants fabrication technologies.

Key technologies are in hand establishment in representative structures



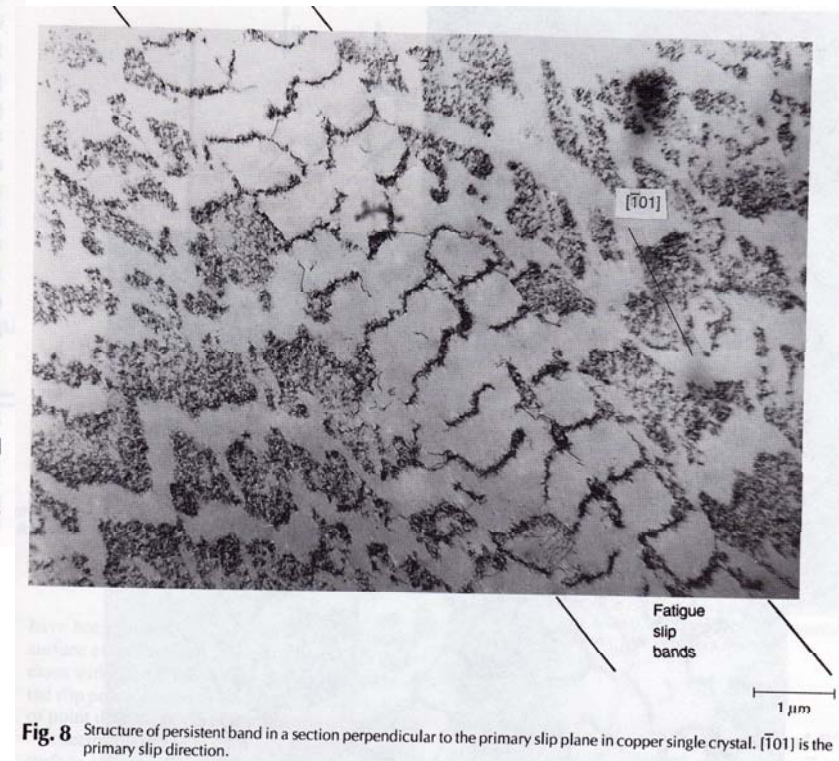
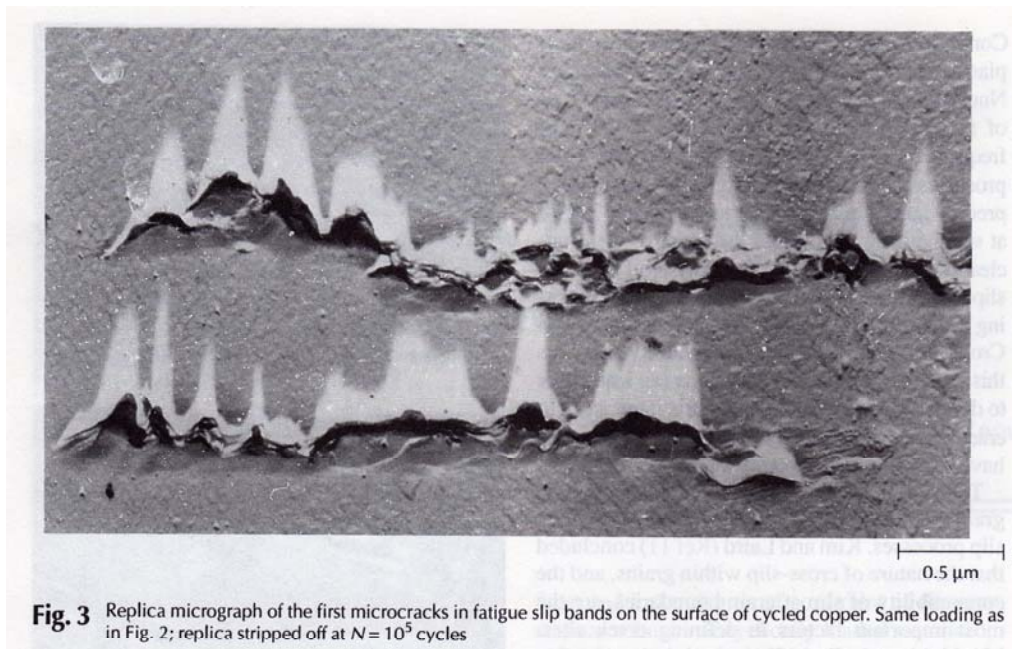
T.Higo/KEK

Outline

- Fabrication of pulse heating samples
 - What determine pulse heating damages**
 - Characteristics of copper and alloys
 - Plan for small damage single cell SW structure fabrication
- Studies on toward perfect copper surface
 - What determine β (field enhancement factor)**
 - Apply semi-conductor technologies
 - High temperature annealing
 - In-situ removing CuO/Cu₂O by He ion
 - Plan for low β ($20 <$) single cell SW structure fabrication
- Future studies of cost effective mass production
 - 1 dollar disk fabrication -> G.Law (SLAC)/~1988**
 - Structure fabrication procedure at NLC/GLC
 - Status of high precision diamond tuning and 3D milling technologies
 - A disk auto loading system on the diamond turning machine

Fatigue slip band on the surface of cycled copper

ref: ASM Handbook



Crack nucleation

ref: ASM Handbook

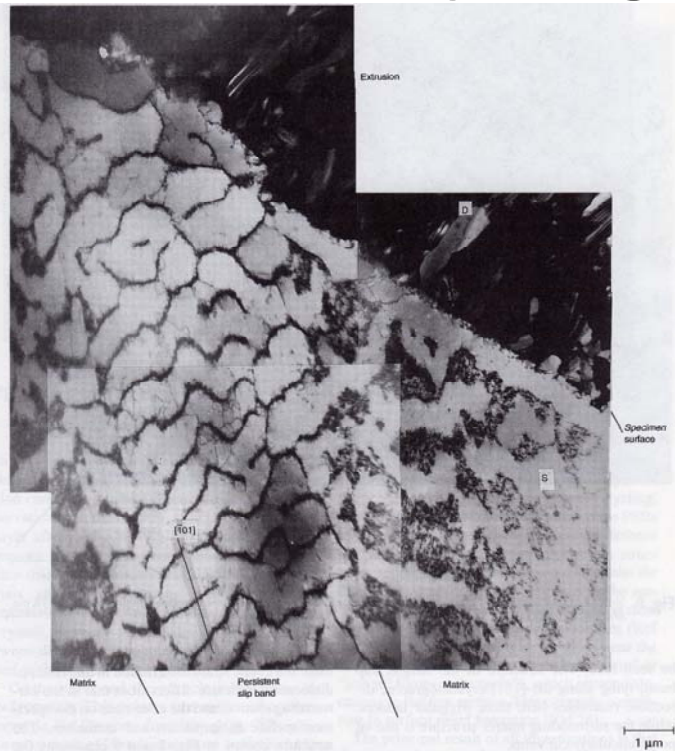


Fig. 9 Surface relief and underlying dislocation structure in a section perpendicular to the specimen surface and the primary slip plane in copper single crystal. D, electrodeposited layer; S, specimen TEM

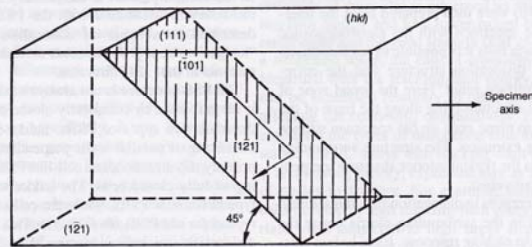


Fig. 10 Notation of crystallographic planes and directions

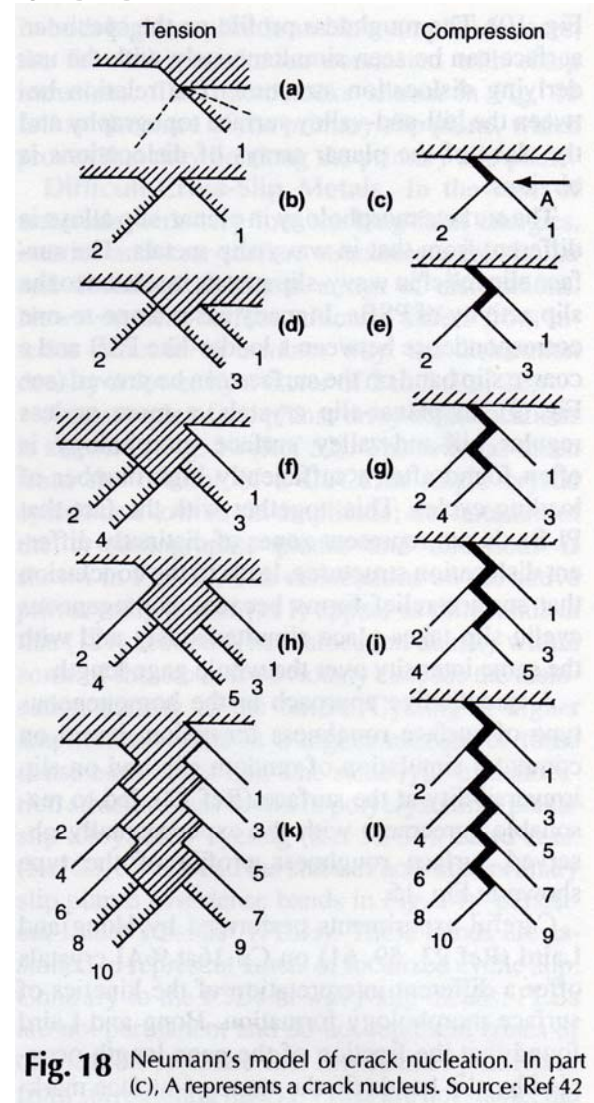
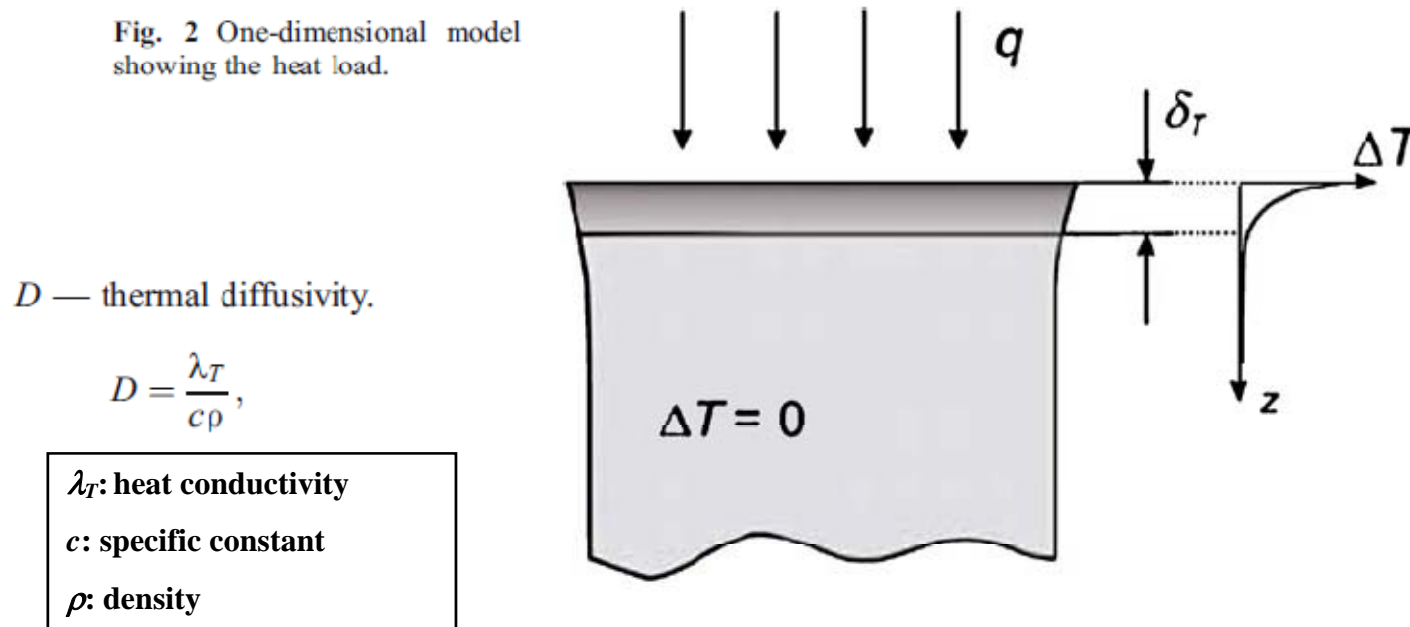


Fig. 18 Neumann's model of crack nucleation. In part (c), A represents a crack nucleus. Source: Ref 42

Fig. 2 One-dimensional model showing the heat load.



In our case the heating of the surface is caused by a magnetic field which penetrated inside the RF skin layer of the metal. Thus, equation (4) can be rewritten using the tangential component of the magnetic field H_τ as follows:

$$\Delta T_{\max} = \sqrt{\frac{D\tau}{\pi}} \frac{1}{\lambda_T} \sqrt{\frac{\mu_0 \omega}{2\sigma}} H_\tau^2, \tag{6}$$

where μ_0 is the permeability of the vacuum, ω — RF frequency, σ — specific conductance

In order to study an irreversible destruction of the surface due to pulsed heating, we will analyze the evolution of the metal surface's microstructure. We will start with the analysis of the copper crystal structure. The ideal copper crystal has a face-centered cubic lattice, where any atom is linked to the neighboring one (Fig. 3). The probability to break any of these links (probability to create an empty vacancy) for this lattice is well-known:

$$p_j = \exp\left(-\frac{U_c}{k_B T_c}\right), \quad (7)$$

Here U_c — is an average energy of the coupling between neighboring atoms, T_c is a steady state temperature and k_B is a Boltzman's constant. If $T_c > 0$, the probability is nonzero and broken links occur every time; therefore, the higher the temperature, the higher the probability. However, if the temperature is well below the melting point, the value of p_j is rather small. This condition is shown next:

$$\frac{U_c}{k_B T_c} \gg 1. \quad (8)$$

$$p_j = \exp\left(-\frac{U_c - \bar{U}}{k_B T_c}\right), \quad (9)$$

where \bar{U} is the energy of external forces breaking a given link, which is zero when $\Delta T=0$.

where the linear thermal expansion of the individual grain with a typical size of l_0 is:

$$x = \alpha \cdot l_0 \cdot \Delta T, \quad (20)$$

and α is a coefficient of thermal expansion. Defining k , as $k = \frac{ES}{l_0(1-\mu)}$, where $S = \delta_T l_0$, E is Yung's module and μ is Poisson coefficient, we finally get:

$$\bar{U} = \frac{E}{1-\mu} \cdot \frac{\alpha^2 \cdot \delta_T \cdot l_0^2 \cdot \Delta T^2}{2 \cdot n_s},$$

We have presented the theory of the copper surface fatigue induced by pulsed heating due to RF Ohmic losses. For the fixed absolute temperature rise, the different mechanisms appeared to be responsible for the fracturing of the copper surface, depending on the pulse length of the applied fatigue cycle. The aim of our study was not to explain the particular properties of the metal's resistance to the fatigue processes. It was aimed at evaluating a tool which can allow the prediction of the material life time behavior towards an extremely high number of fatigue cycles, provided the experimental data for low statistics is available.

However, certain conclusions and newly discovered effects can be used as a background for practical recommendations:

- For the normal conducting Linear Colliders, the range of RF pulse lengths (10–1000 ns) is of the highest interest. We have shown that the major contribution to the mechanical stresses responsible for the copper surface life time in this range of pulse lengths comes from the interaction between the grains located close to the surface.
- For the identical value of the peak surface temperature rise, the life time will be increased if the pulse length is reduced.
- The sizes of the grains on the surface play an important role – the smaller the grain size, the longer the life time.

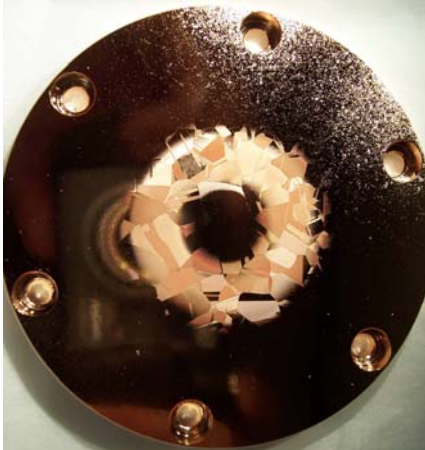
Longer the life time is depend on

0.2,0.5% Stress Strength at high temperature

- Heat conductivity
- Specific constant
- Density
- Poisson coefficient
- Grain size
- Dislocation
- Thermal conductivity
- Thermal diffusivity
- **Electric conductivity**

@ Existing materials (polycrystal, alloy) are complicate

Typical pulse heating samples



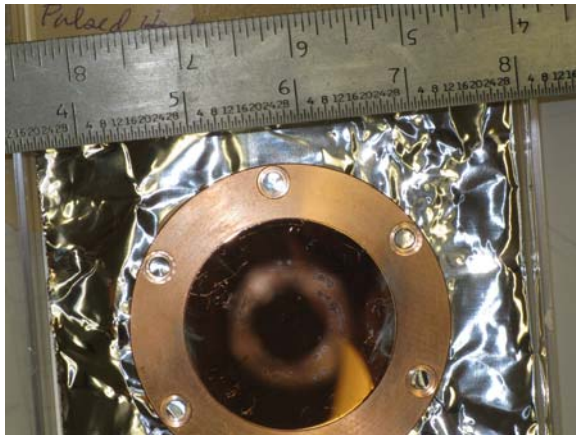
6N



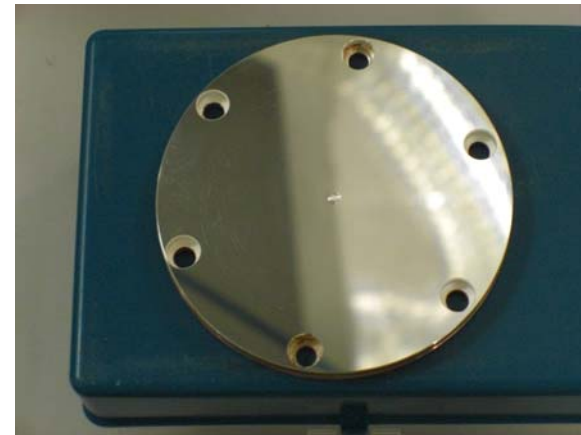
6N/HIP



Electrodeposited Cu



Single crystal Cu (100)



Electrodeposited Ag

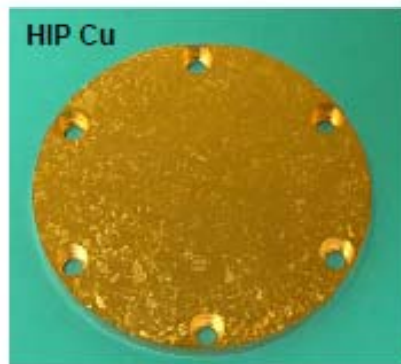
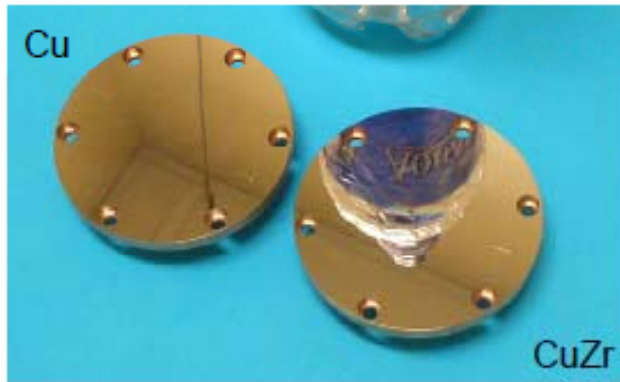
not test yet

2nd Collaboration Meeting on X-band Accelerator Structure Design and Test Program

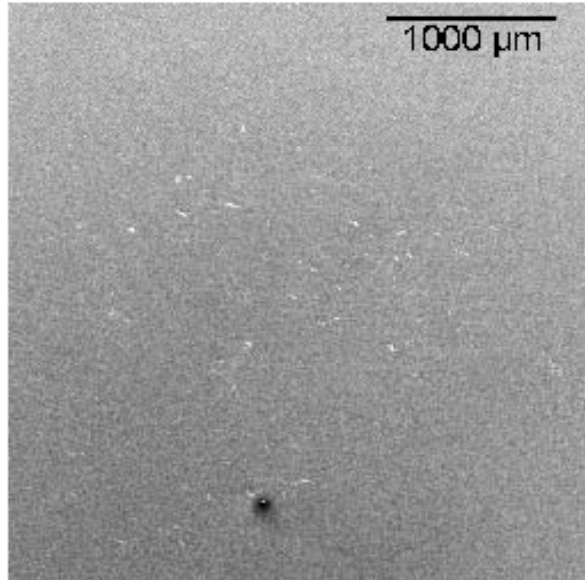
Pulse Heating, Surface Analysis, and Hardness Testing

L. Laurent

SLAC



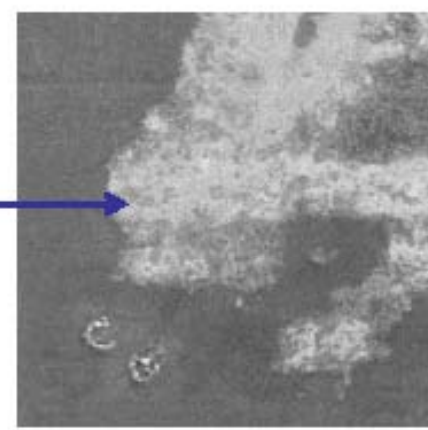
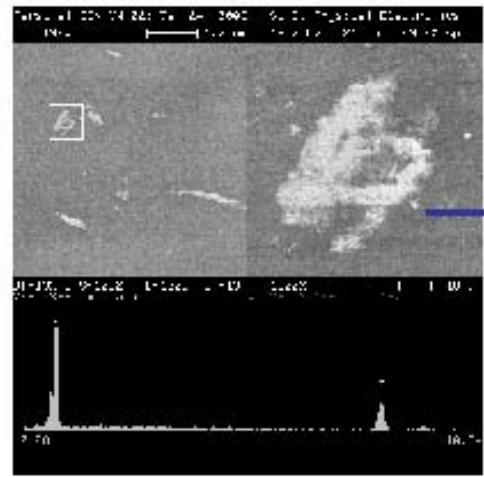
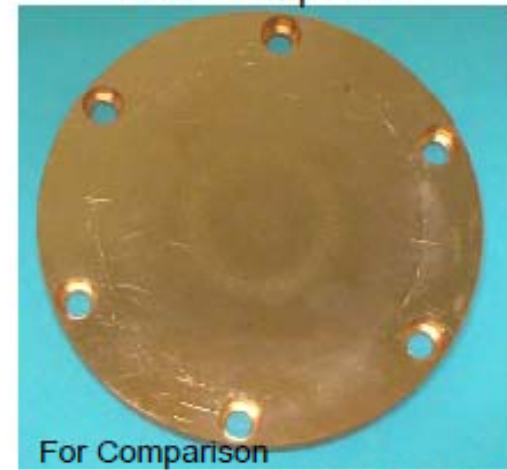
CuZr2



CuZr2: Temp=70°C



Cu1: Temp=70°C



L. Laurent

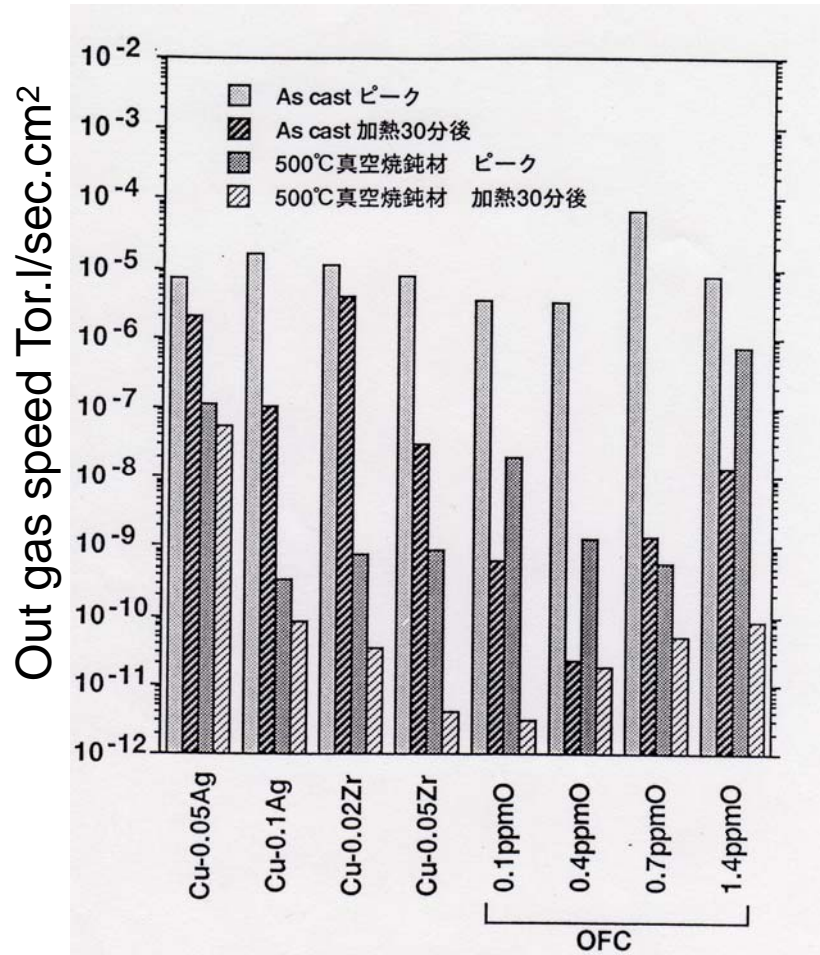
My questions

Why damages are different?

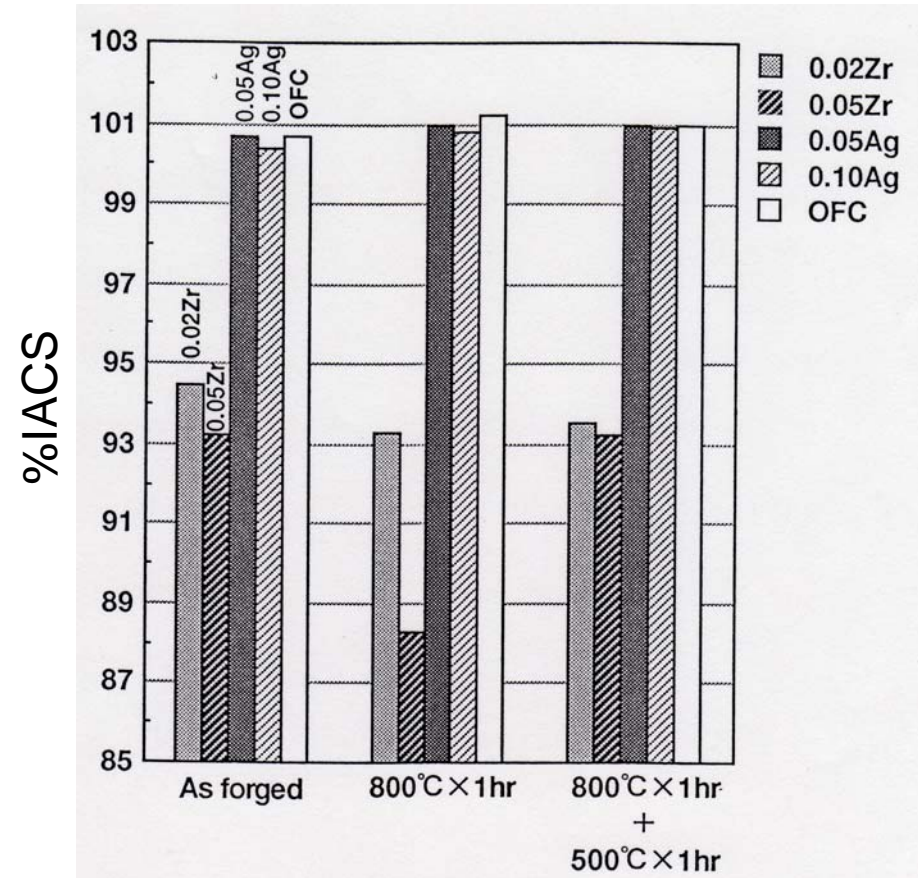
Today!

Focus on mechanical properties of
OFC, CuZr and CuAg

Out gas characteristics and electric conductivity

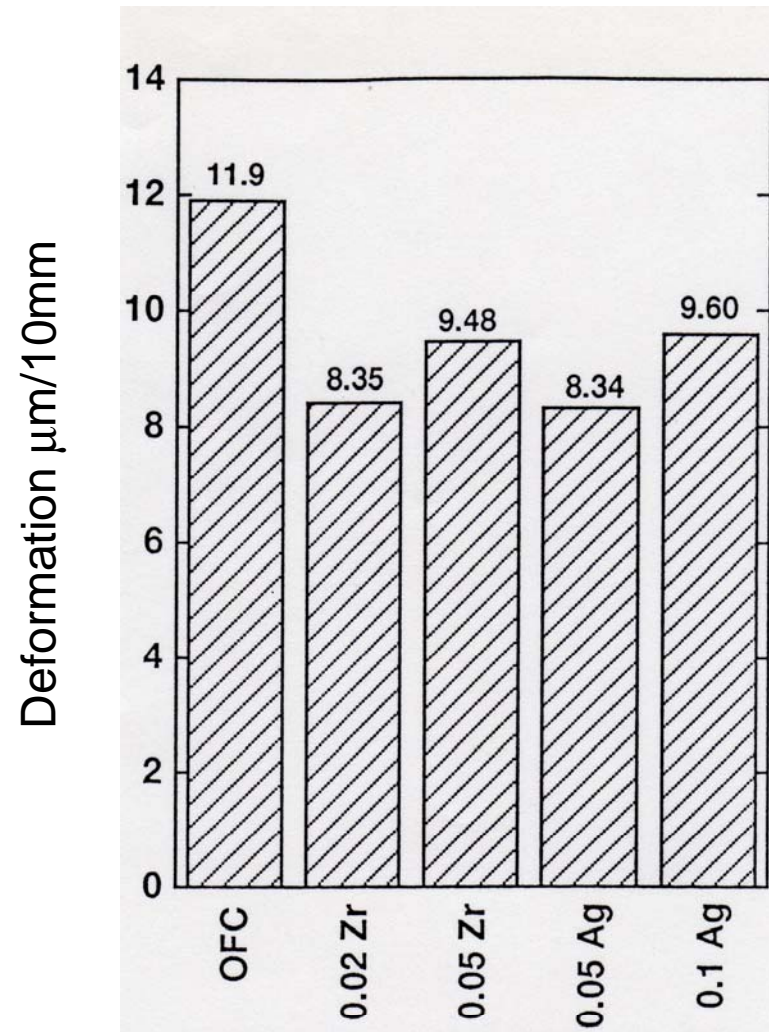


500deC heating under 1×10^{-11} Torr



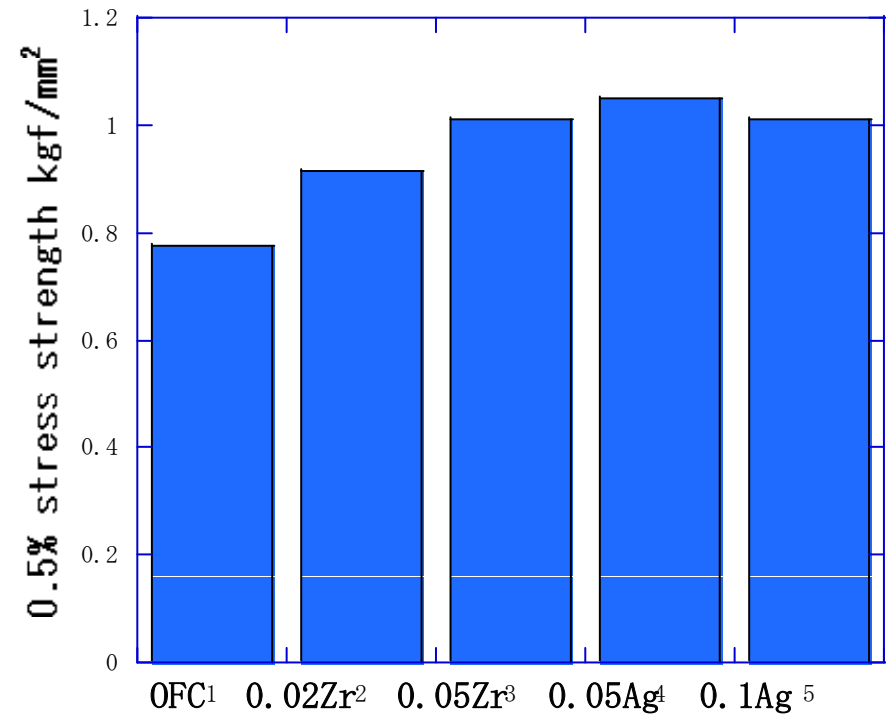
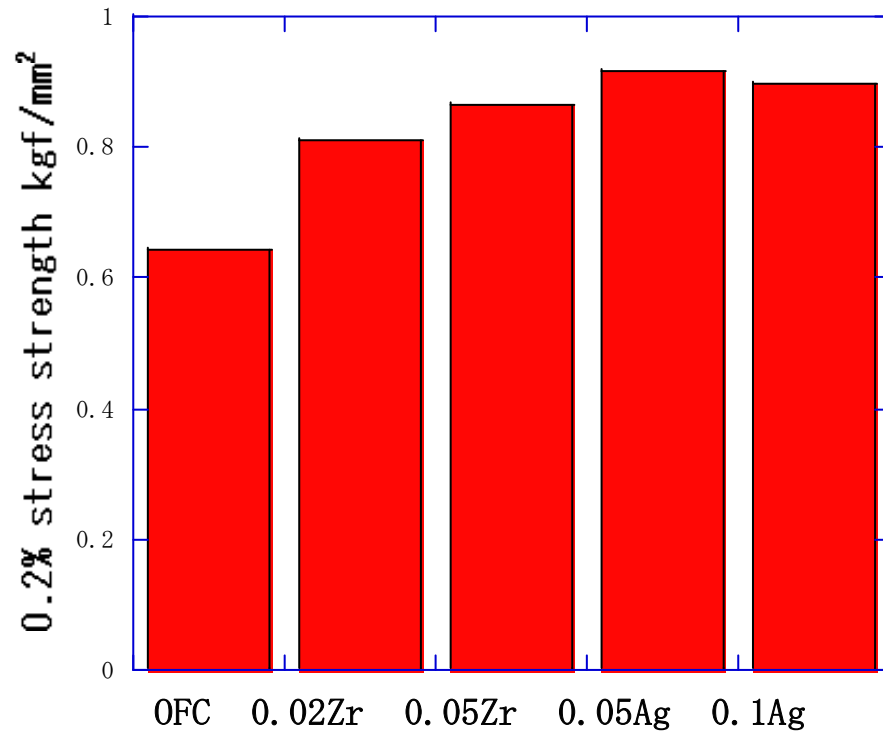
Electric conductivity

Deformation due to 0.1kg/mm² force at 800degC

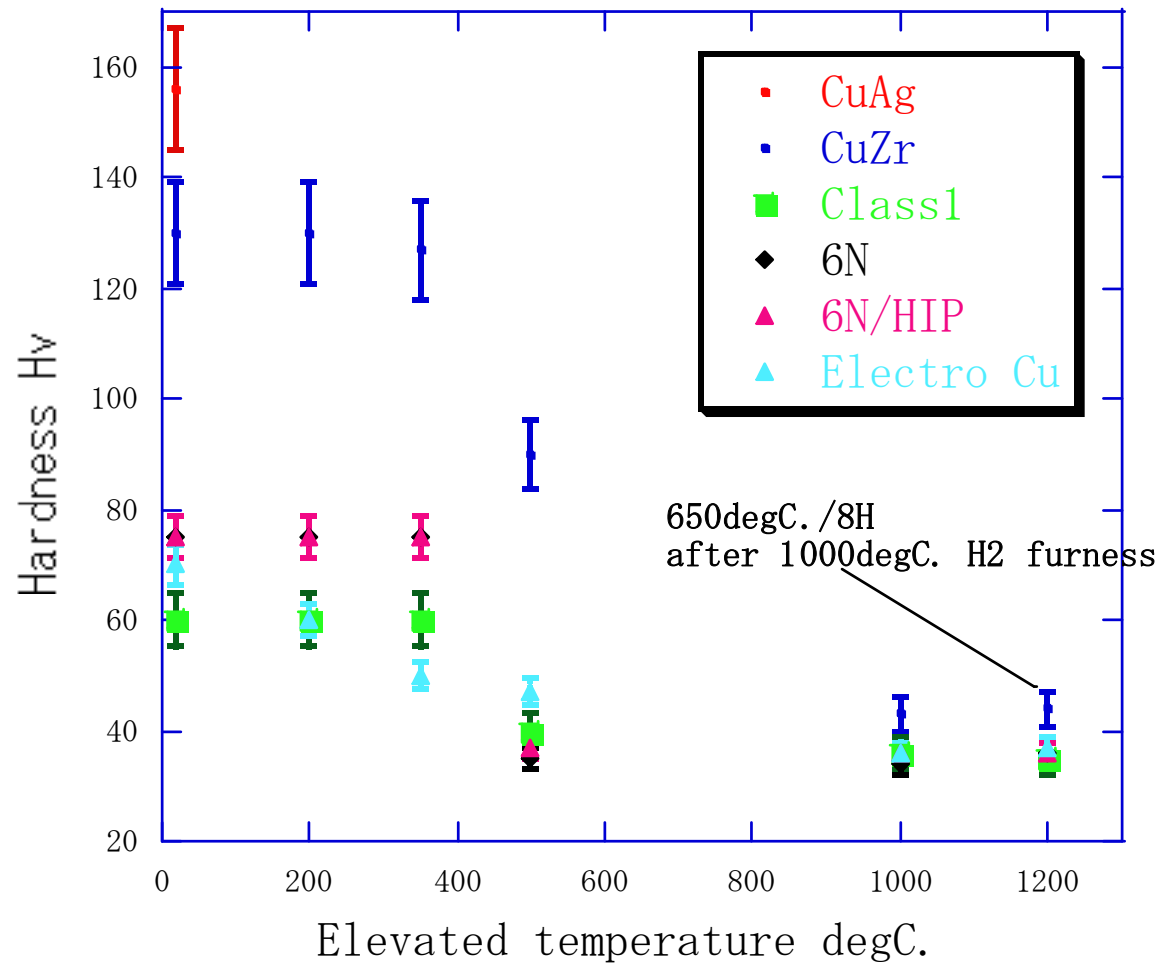


Deformation at 0.01kgf/mm²

0.2%, 0.5% stress strength at 800 degC



Hardness change due to temperature



Effective material

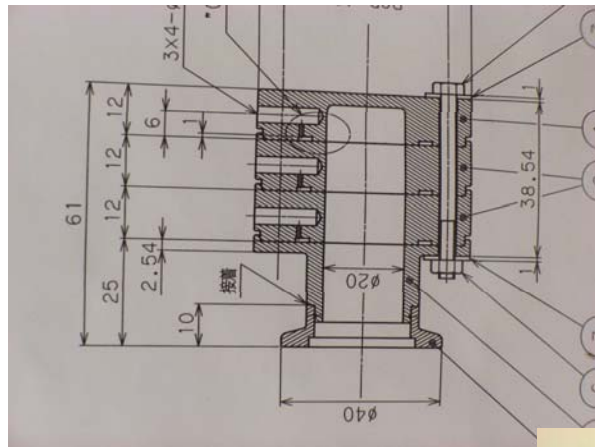
OFC < CuZr < CuAg ??????

BUT

Purity, Grain size, surface stress due to machining are open questions.

Low temperature bonding/rf contact test for CuZr /CuAg

Indium: melting point 156.4 drg.C



Vacuum furnace

No leak has found



Breakdown Studies

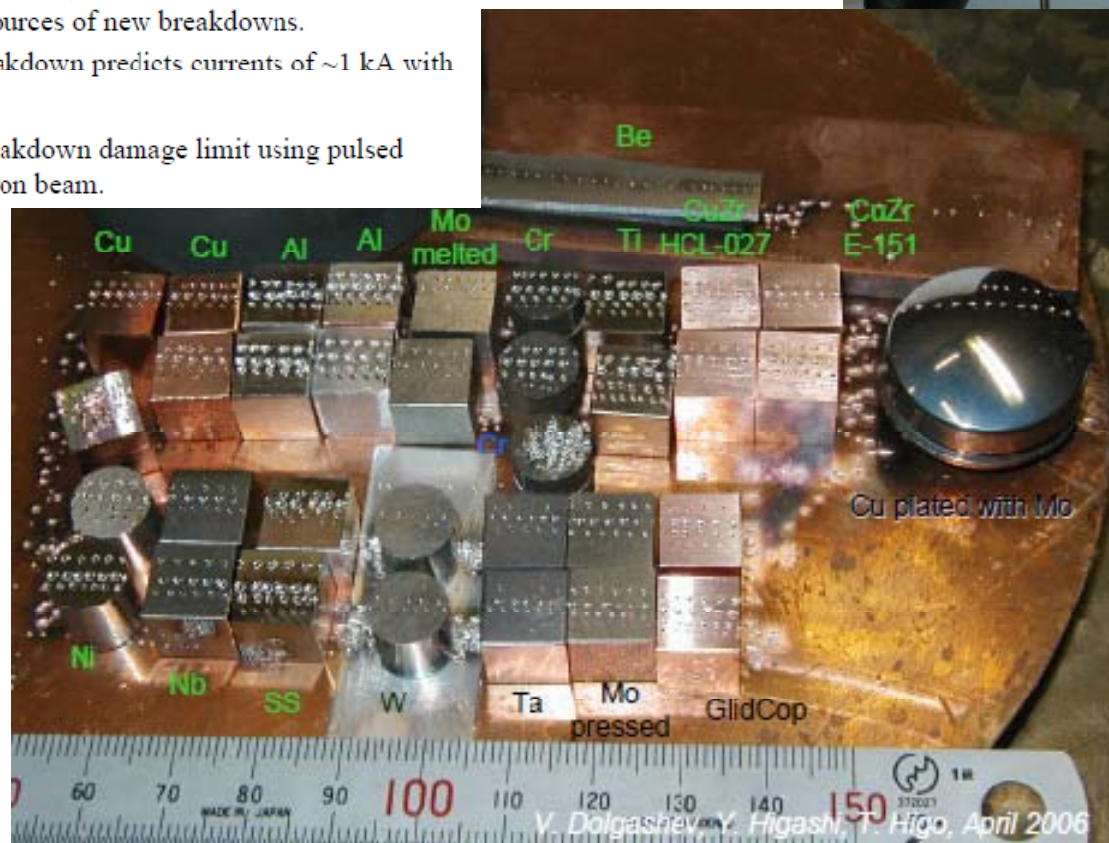
Experiment on Metal Surface Damage Using 120 keV Beam

V.A. Dolgashev (SLAC), Y. Higashi and T. Higo (KEK)

Motivation

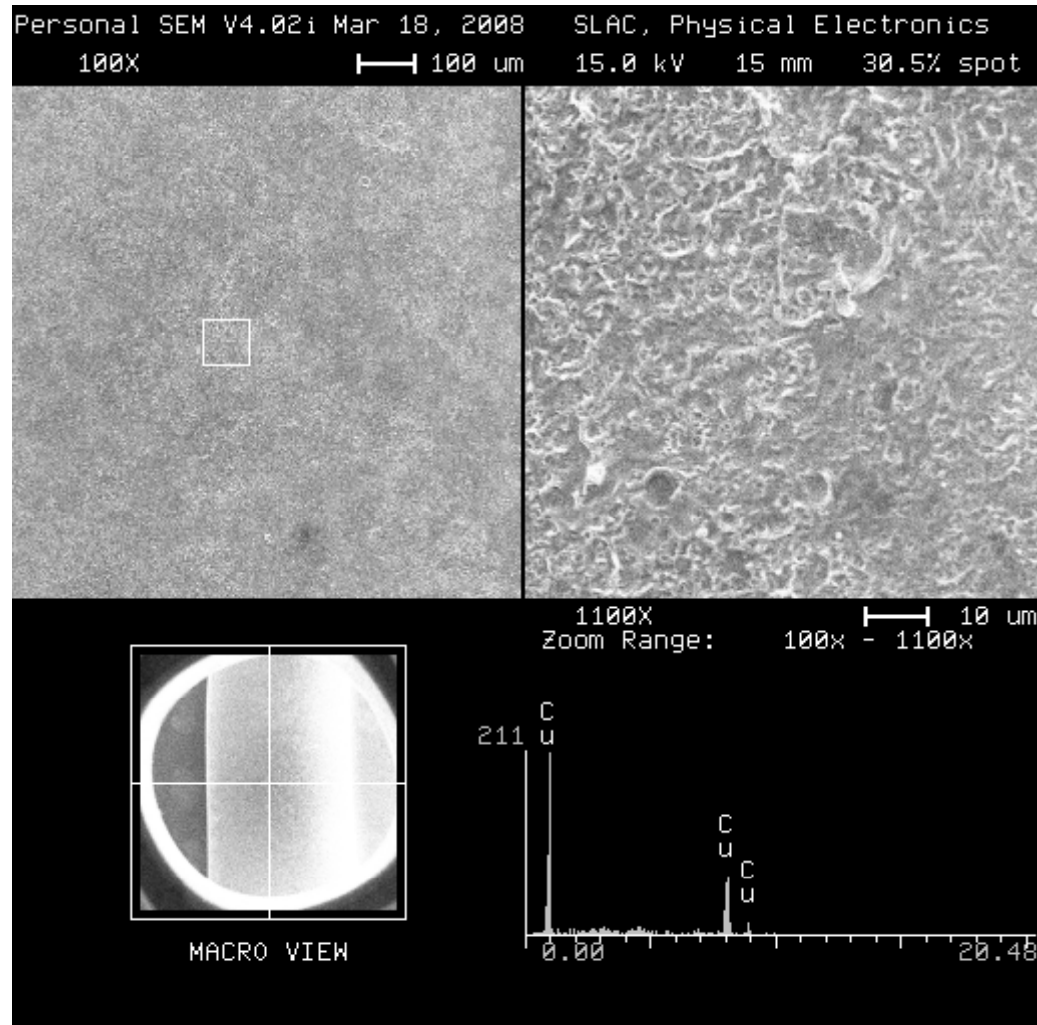
- **Model of rf breakdown damage limit:** arc electron currents heat bulk metal, metal surface melts and then ablates creating sources of new breakdowns.
- Simulation of breakdown predicts currents of ~ 1 kA with energy ~ 100 keV.

Idea: Simulate breakdown damage limit using pulsed 100 keV DC electron beam.

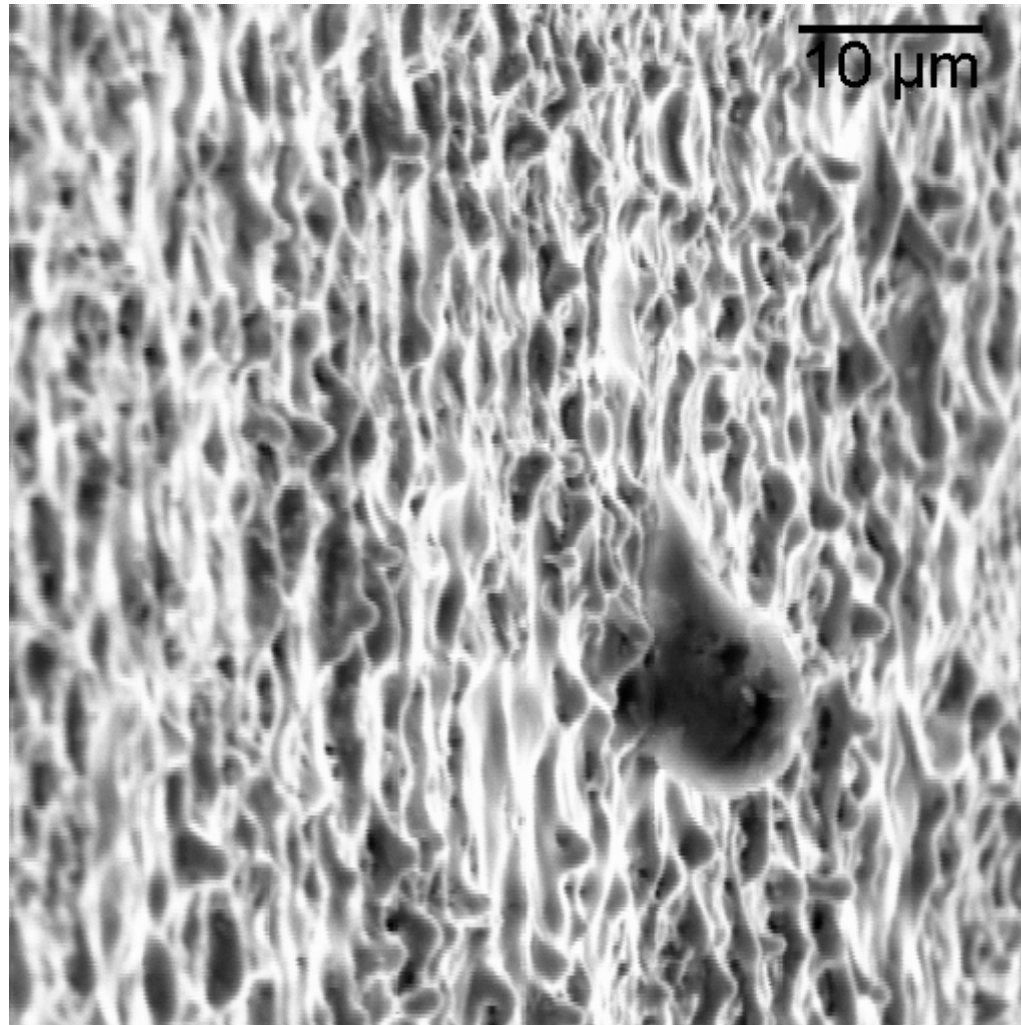


Typical breakdown damage profile (Case 1)

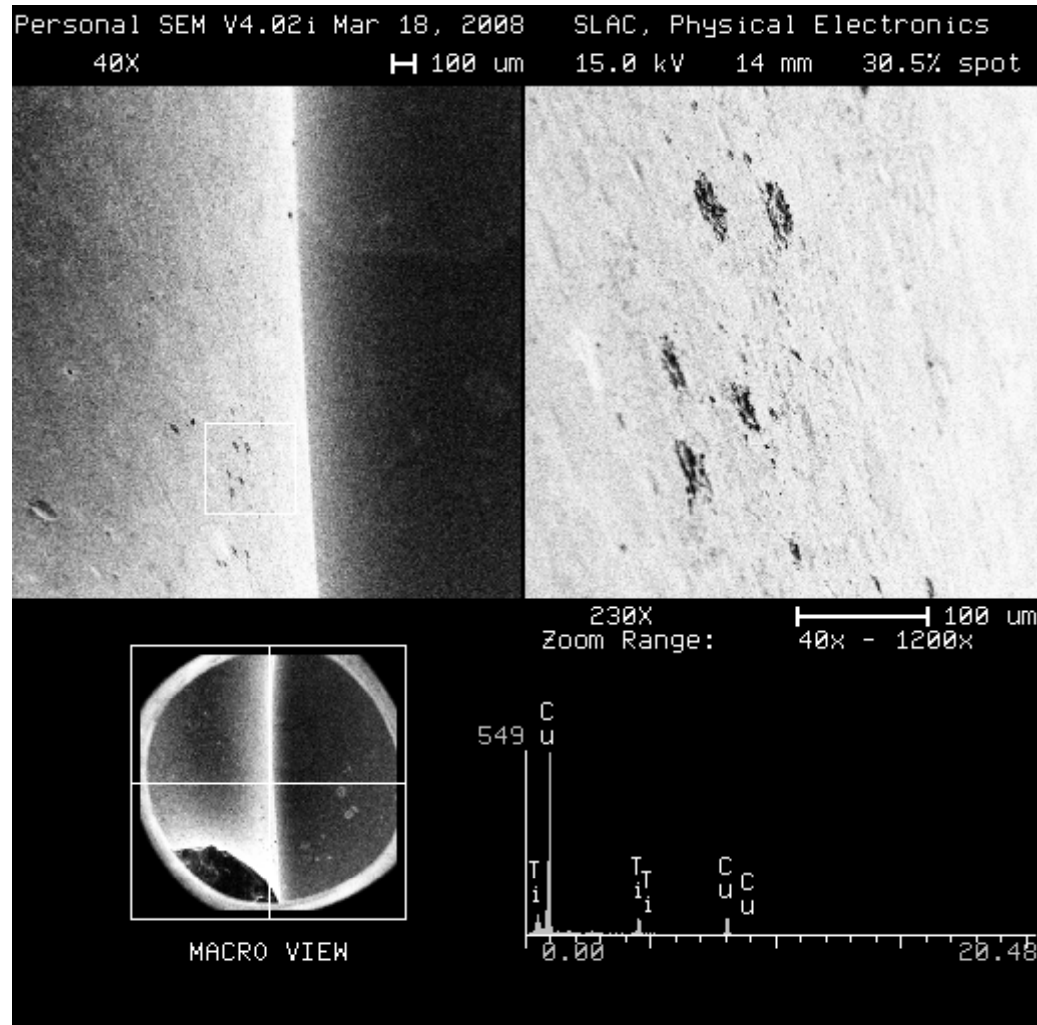
BA-IRS7



CB-IRS-4

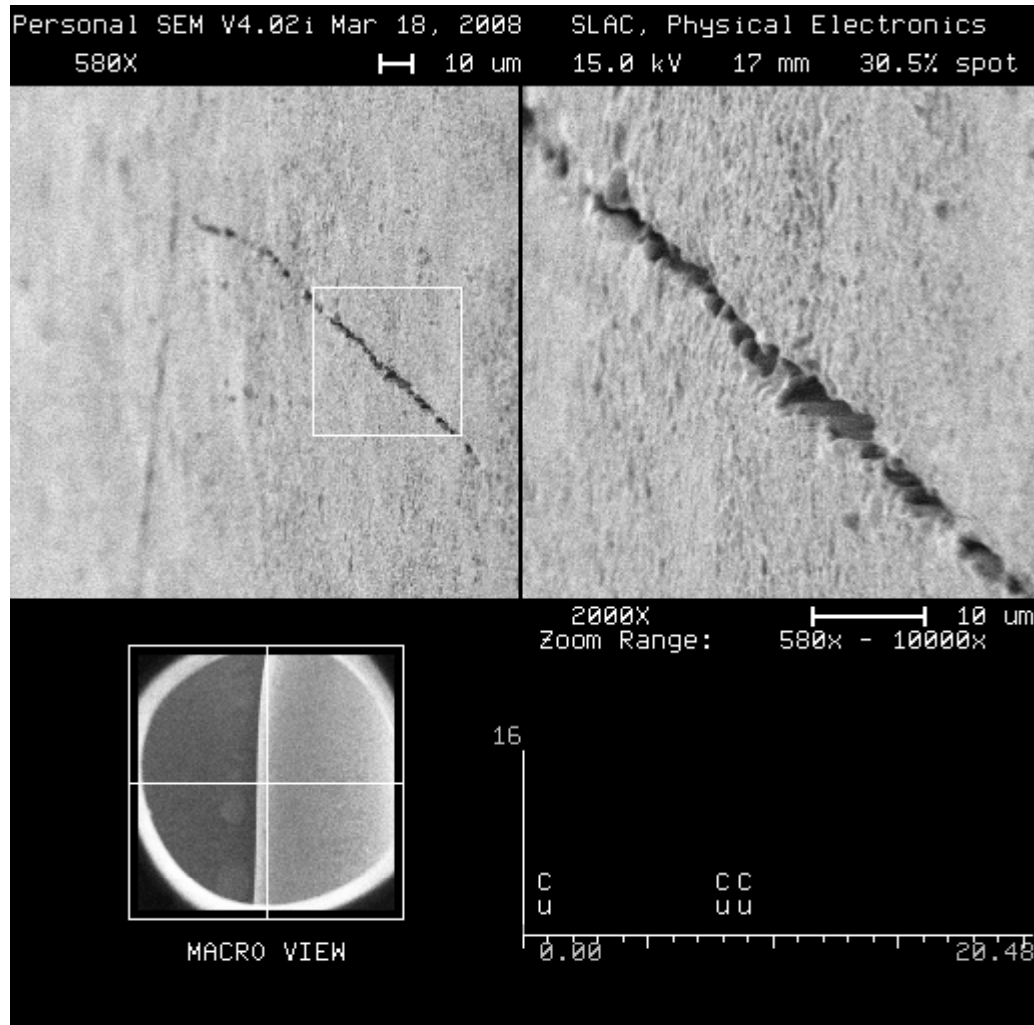


BA-IRS9

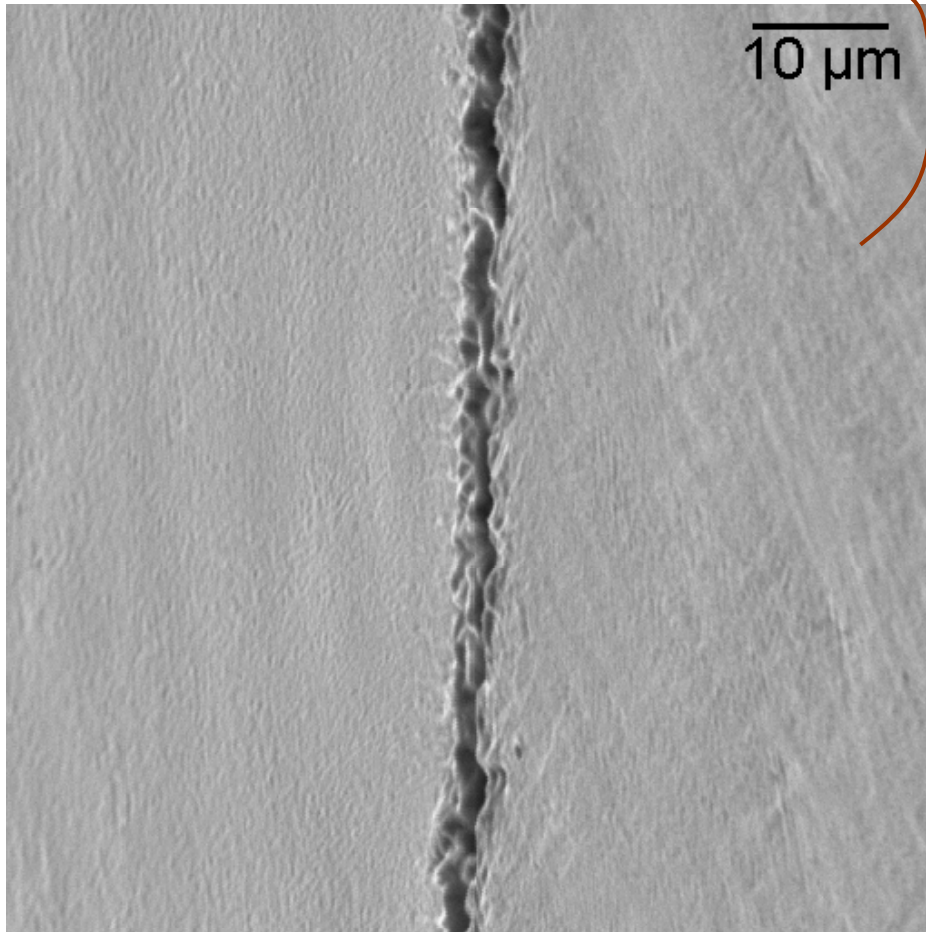
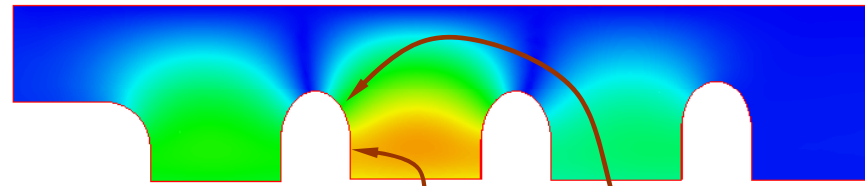


(Case 2)

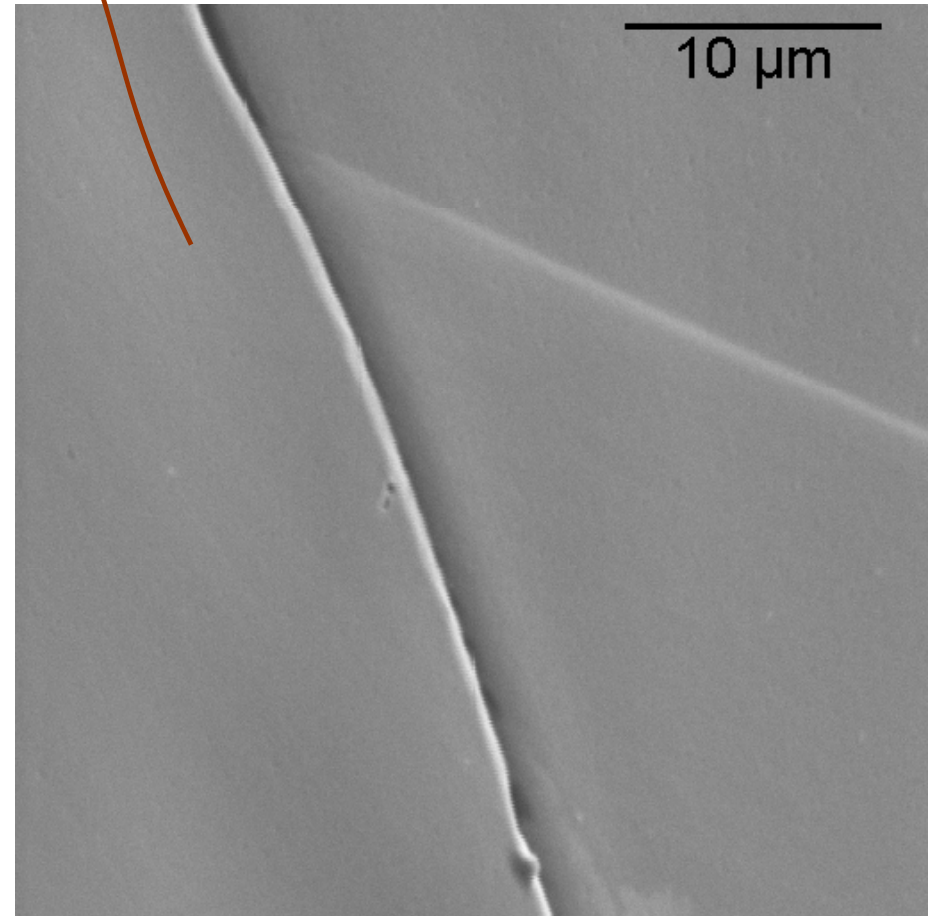
BA-IRS5



Grain boundary on iris of high-gradient cell

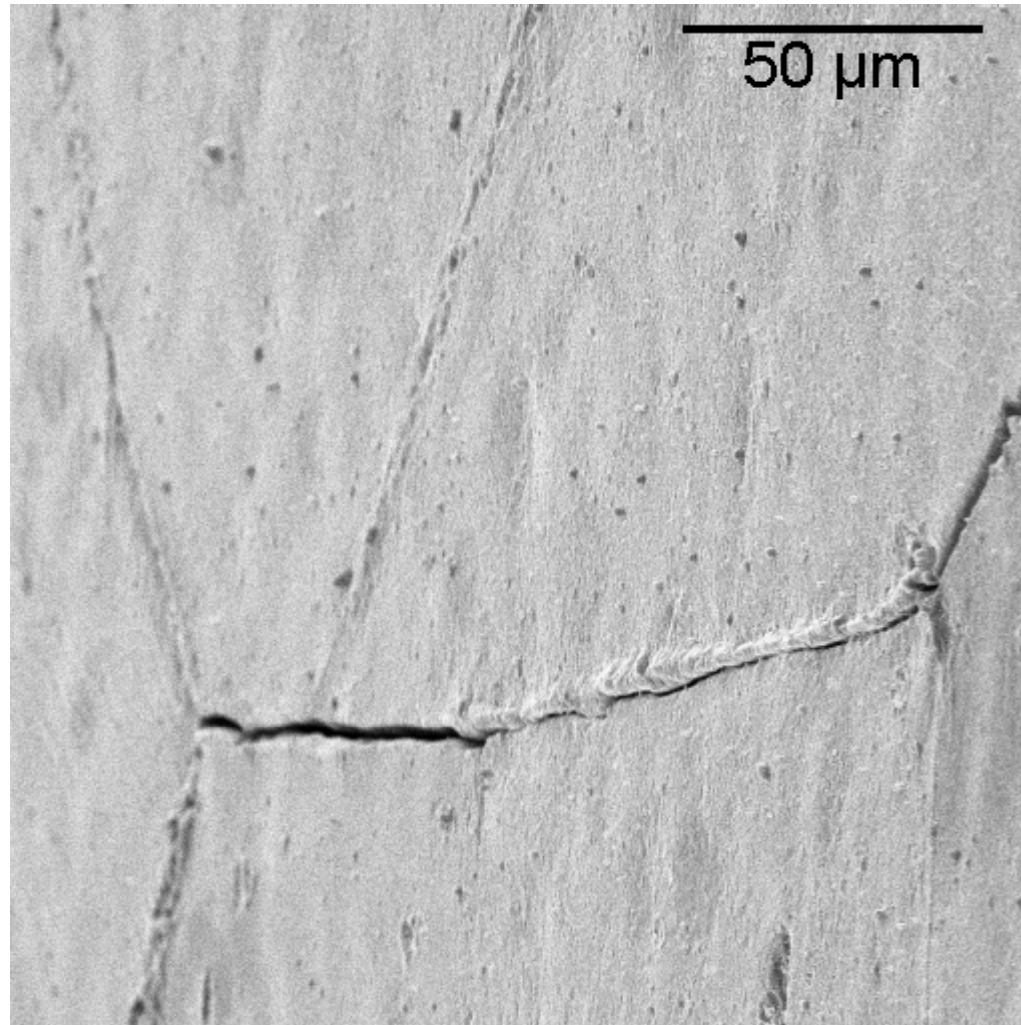


Grain boundary in high **magnetic** field area

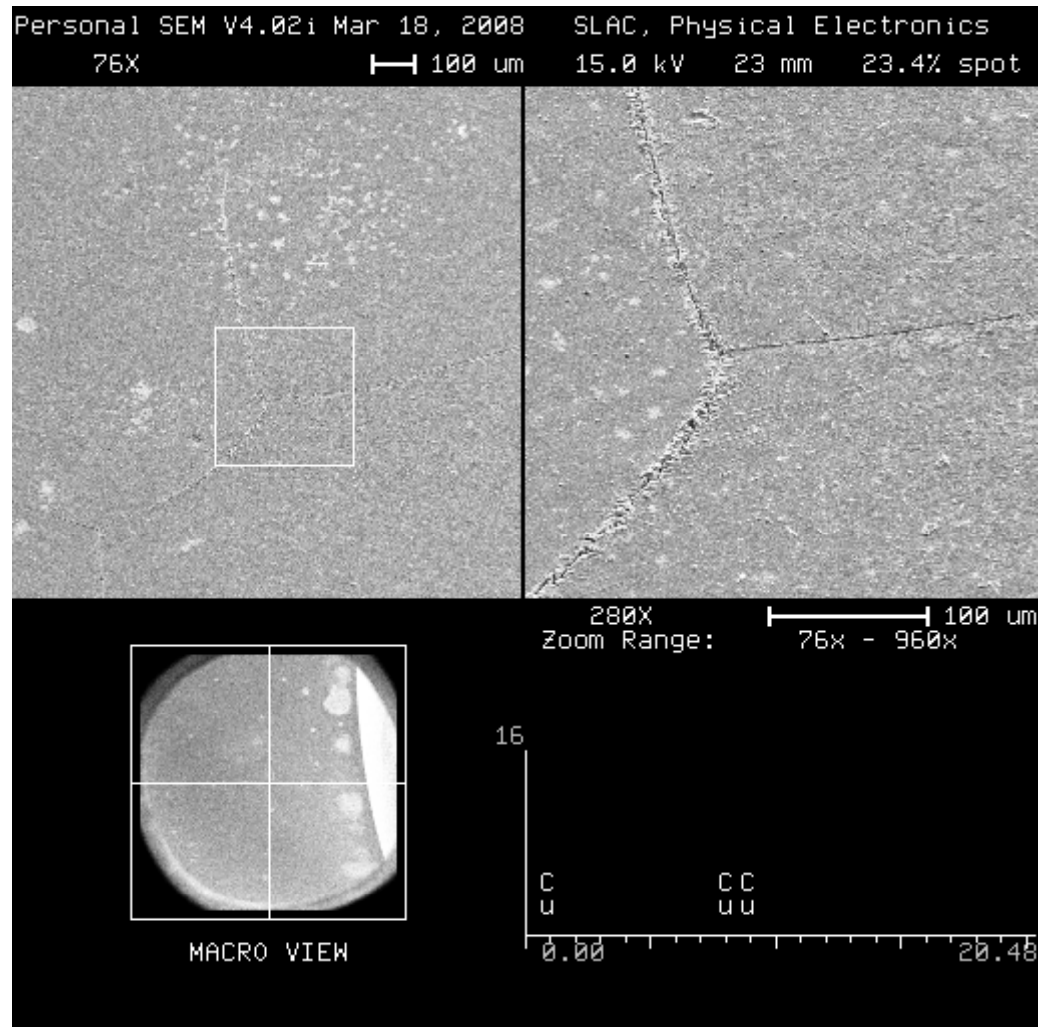


Grain boundary in high **electric** field area

B-WALLE2

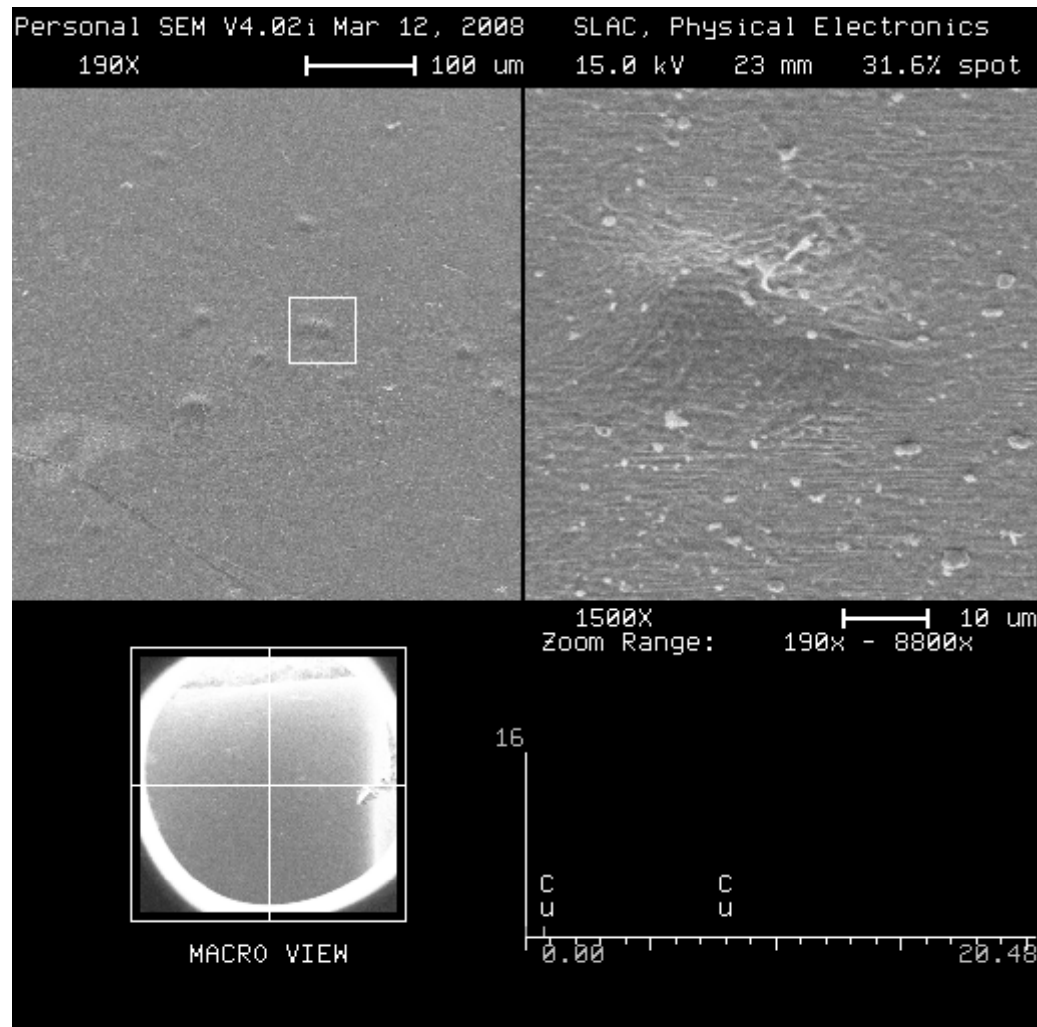


B-Well6



(case 3)

B-BMPS



Surface preparation

- Dust free surface → Done, but conform again
- Reducing Out gas
- Stress free surface
- Copper oxide surface
- Grain size/boundary
- Work function measurement
- Scanning field emission microscopy

Catalogs data of Si wafer cleaning by KANTO CHEMICAL CO. Ltd.
We use Frontier Cleaner W-A02

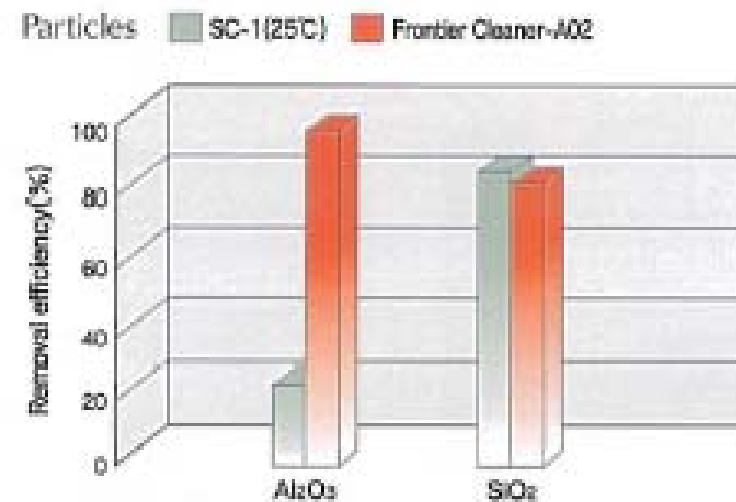
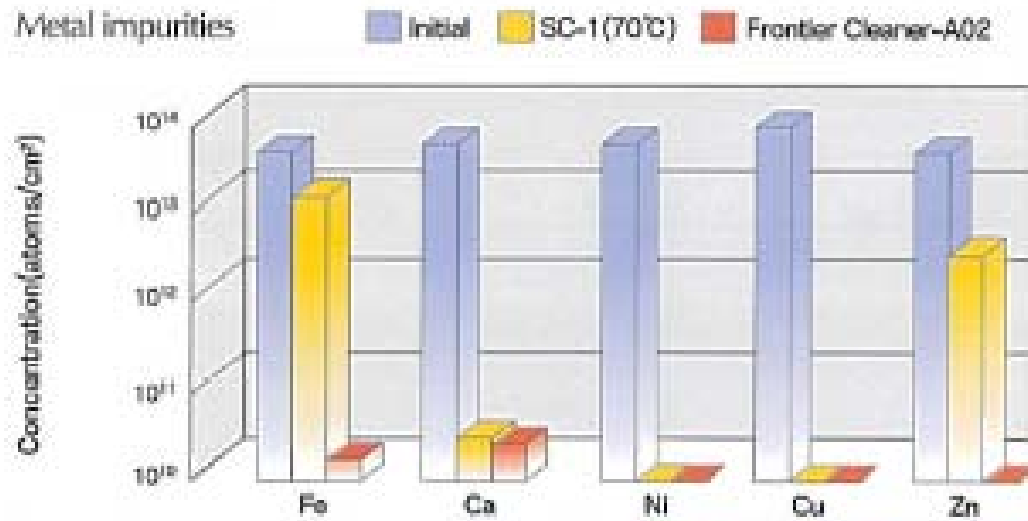
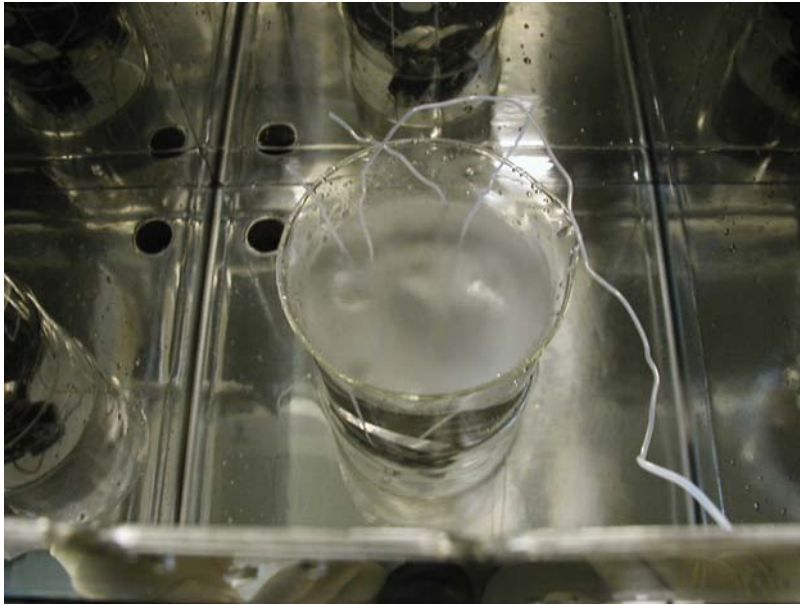
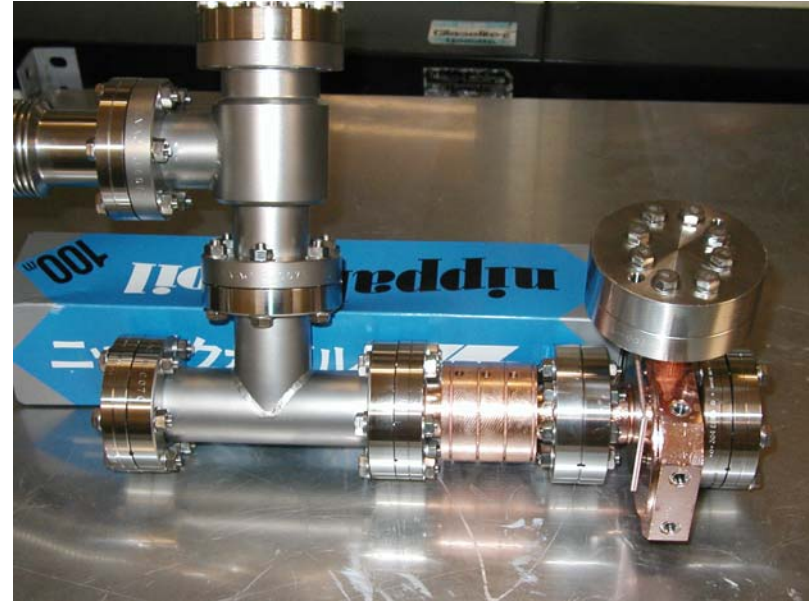


Fig1. Cleaning performance for metal impurities Fig2. Cleaning performance for particles

2nd Single cell SW structure preparation

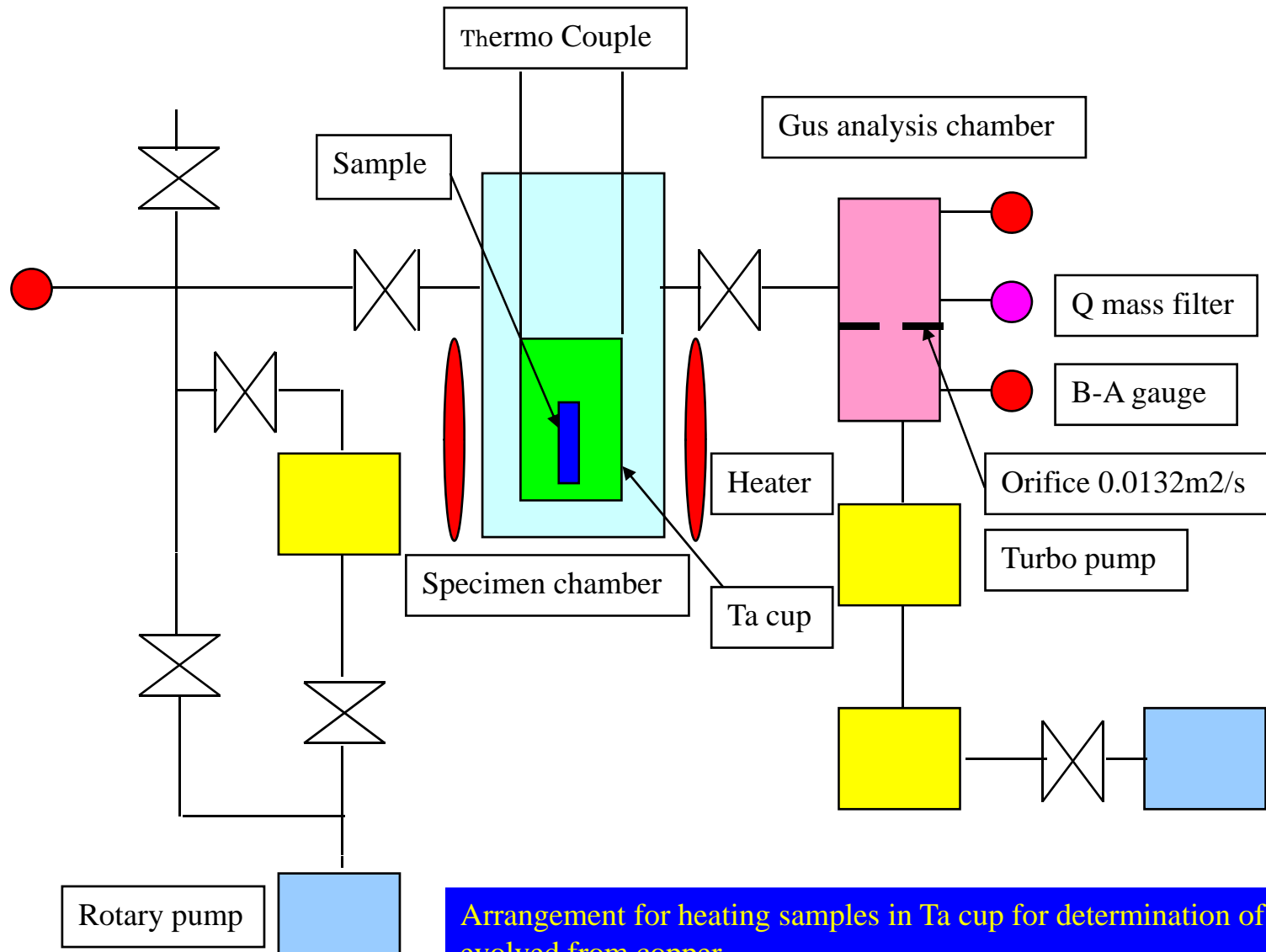


A-02 solution + Megasonic cleaning
960kHz, 600 W, 5 minutes operation
Ultra Pure Water

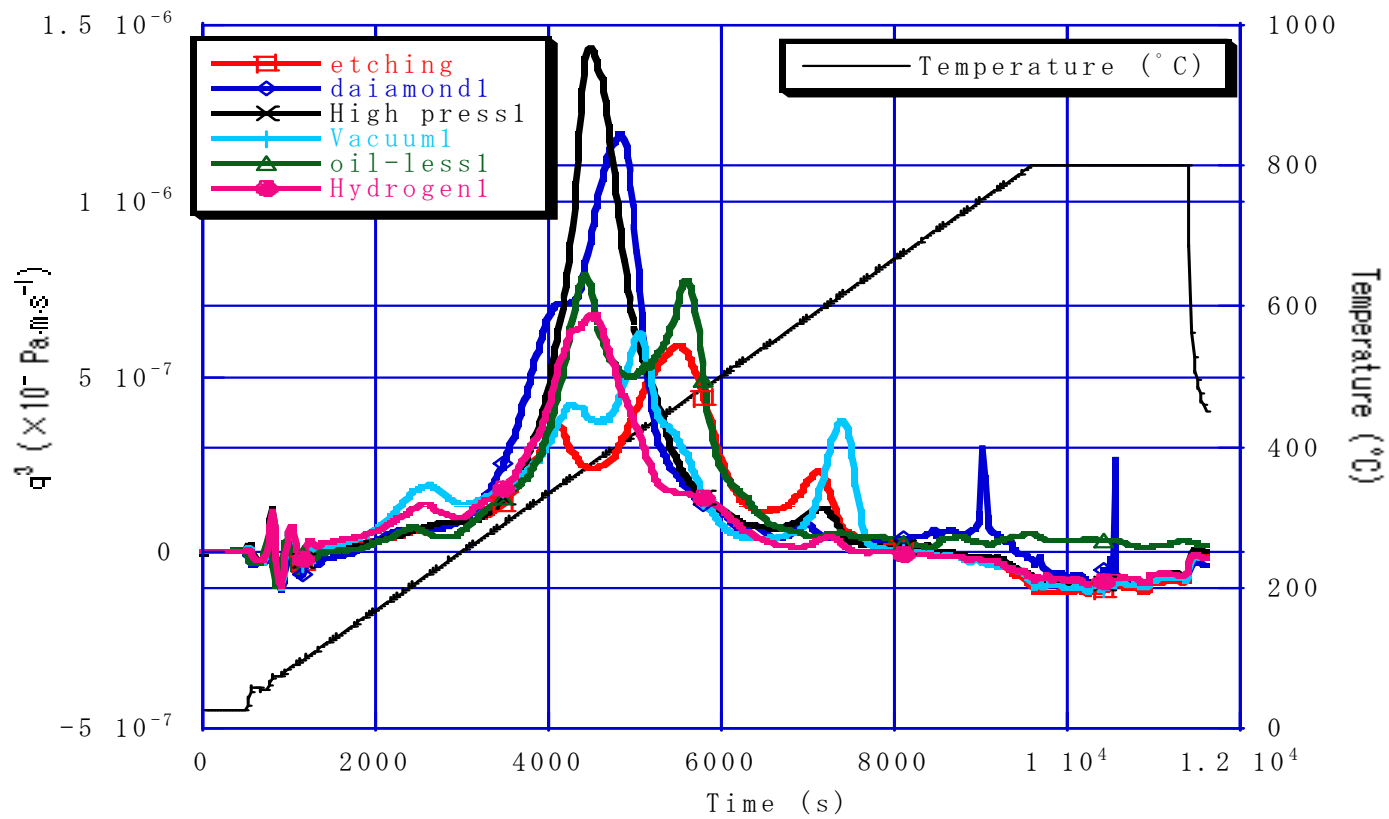


All parts were applied megasonic cleaning
Assemble envelopment: Class 10
No vacuum leak
300 degC baking, period : 5days

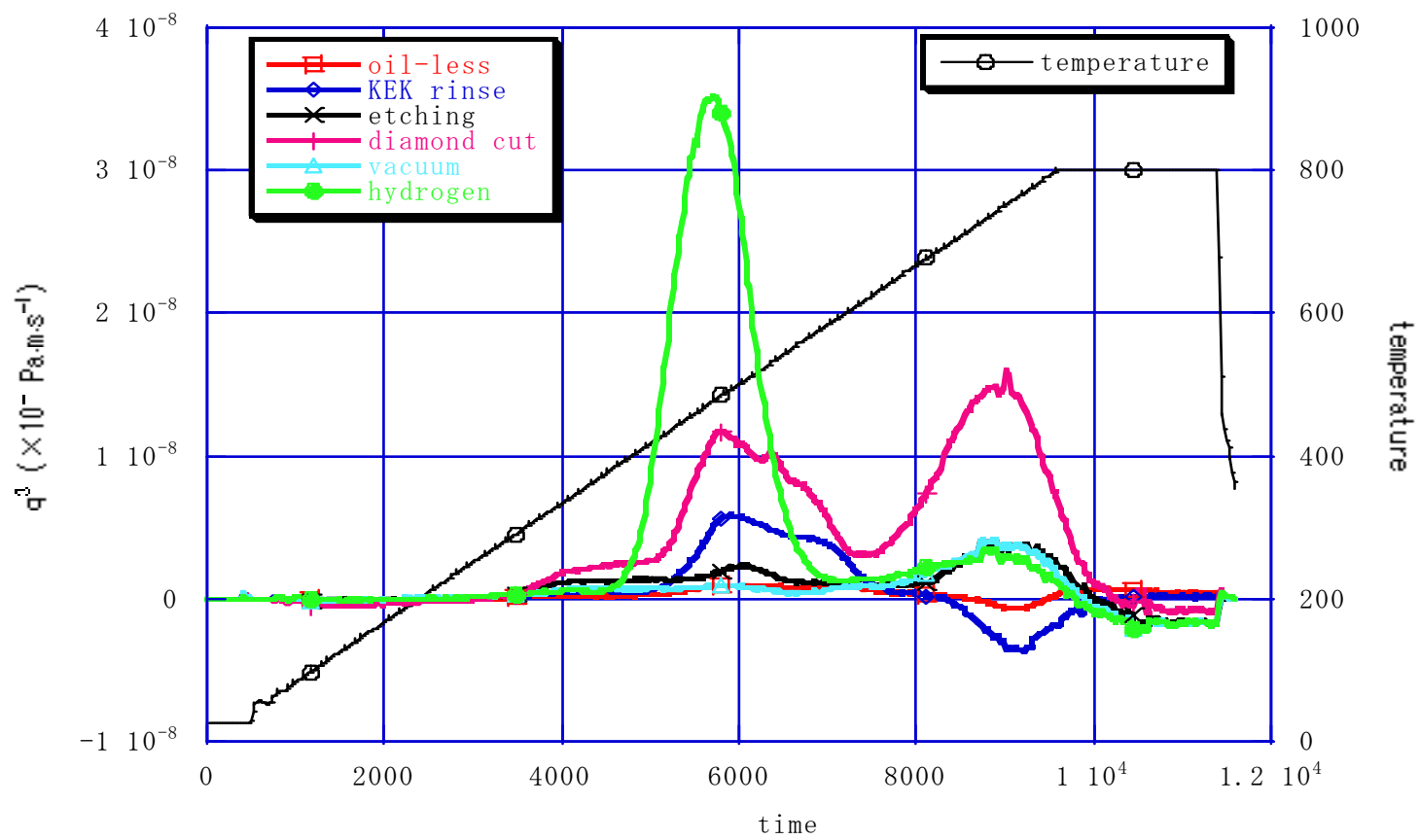
Out gas measurement by TDS



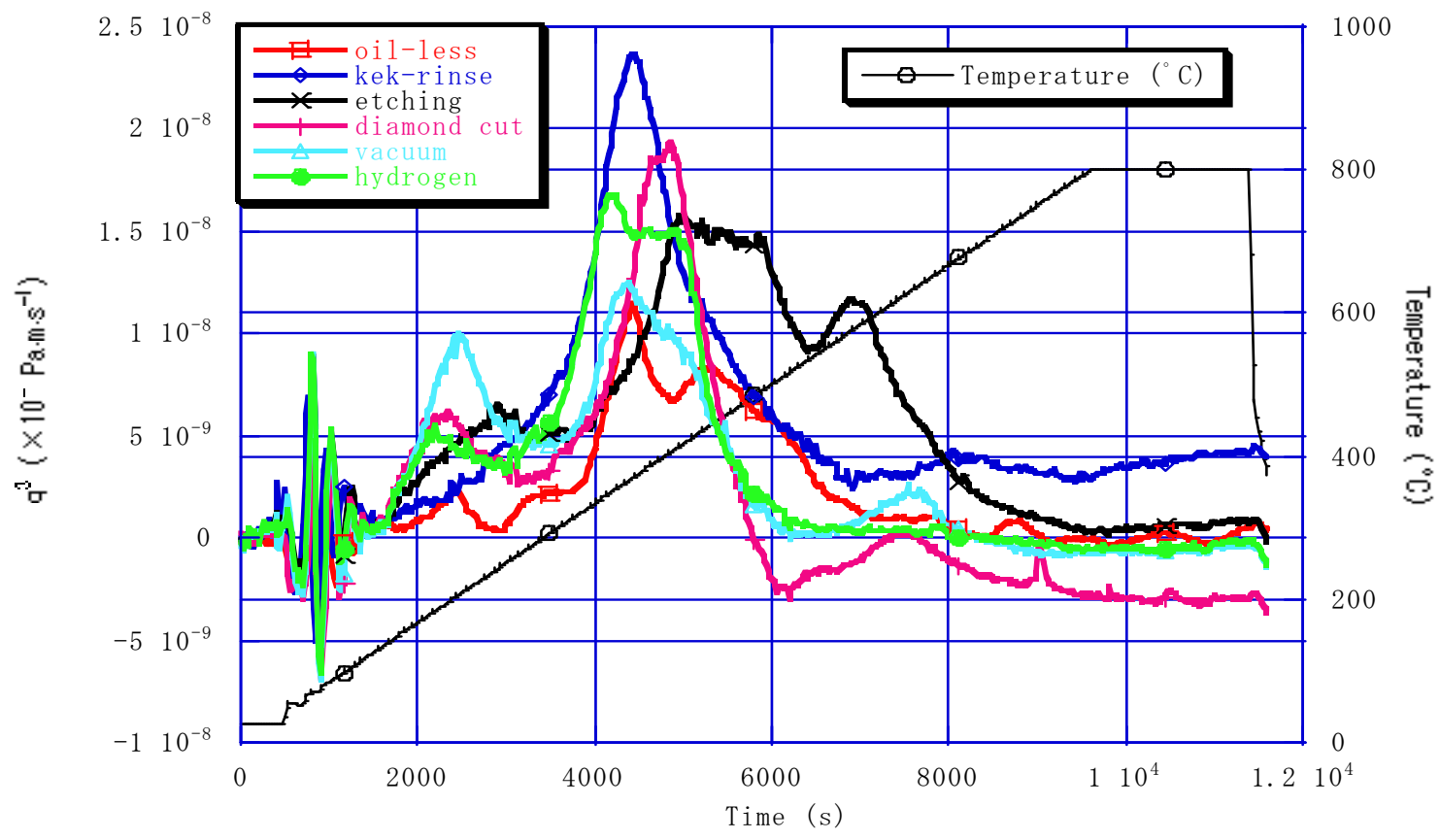
Arrangement for heating samples in Ta cup for determination of gases evolved from copper



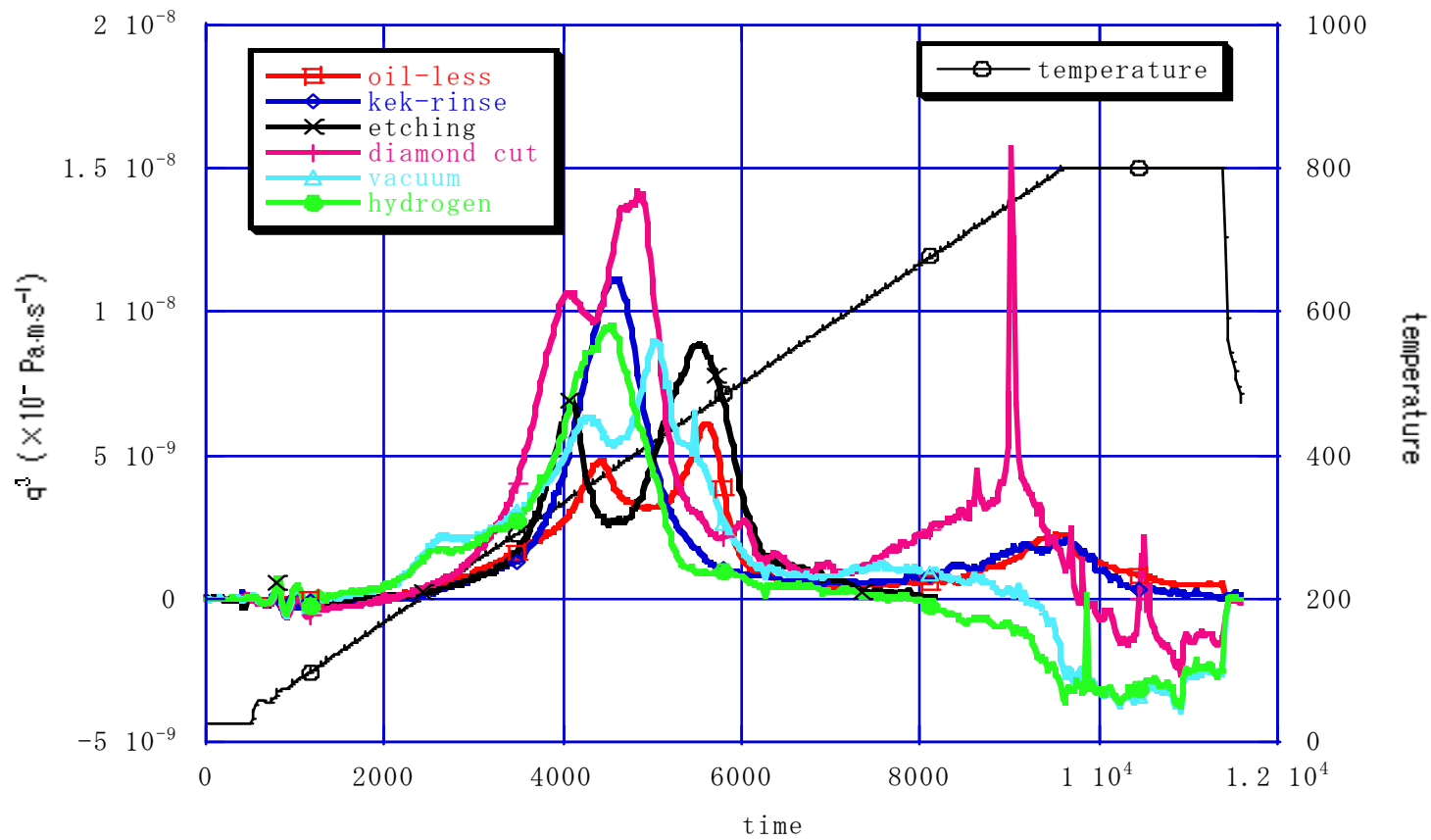
Out gas characteristics on various treatment of OFC



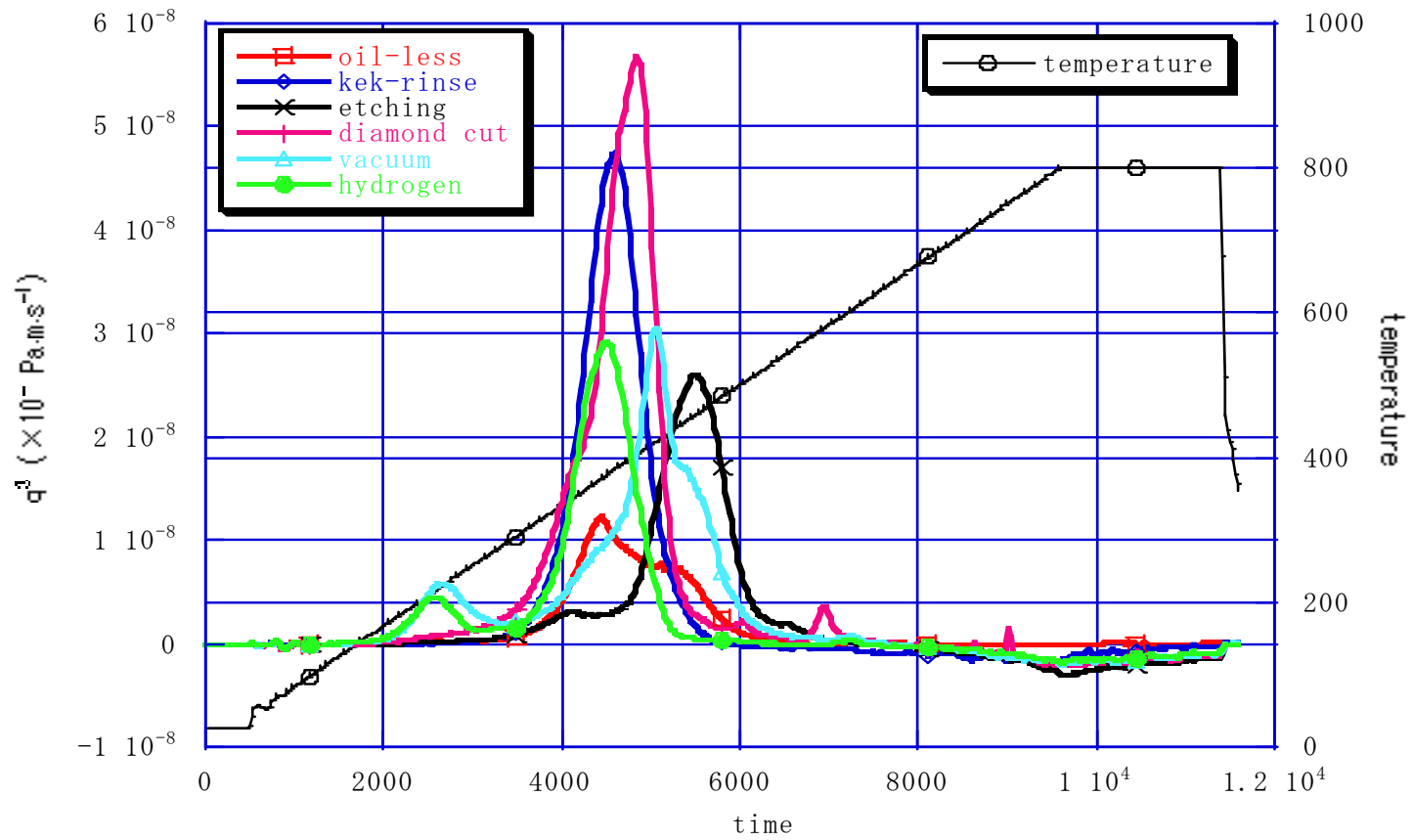
H₂



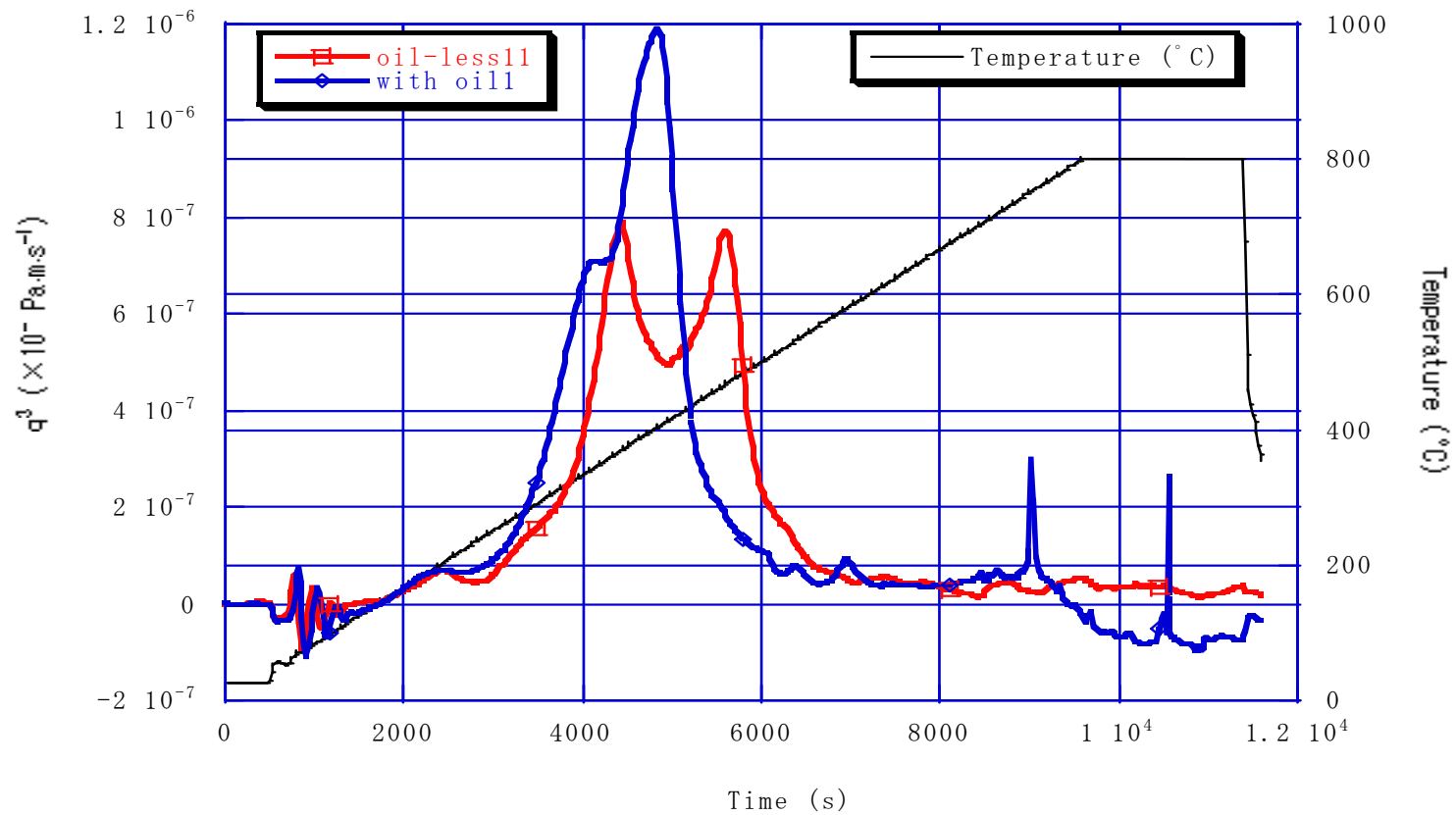
H₂O



CO



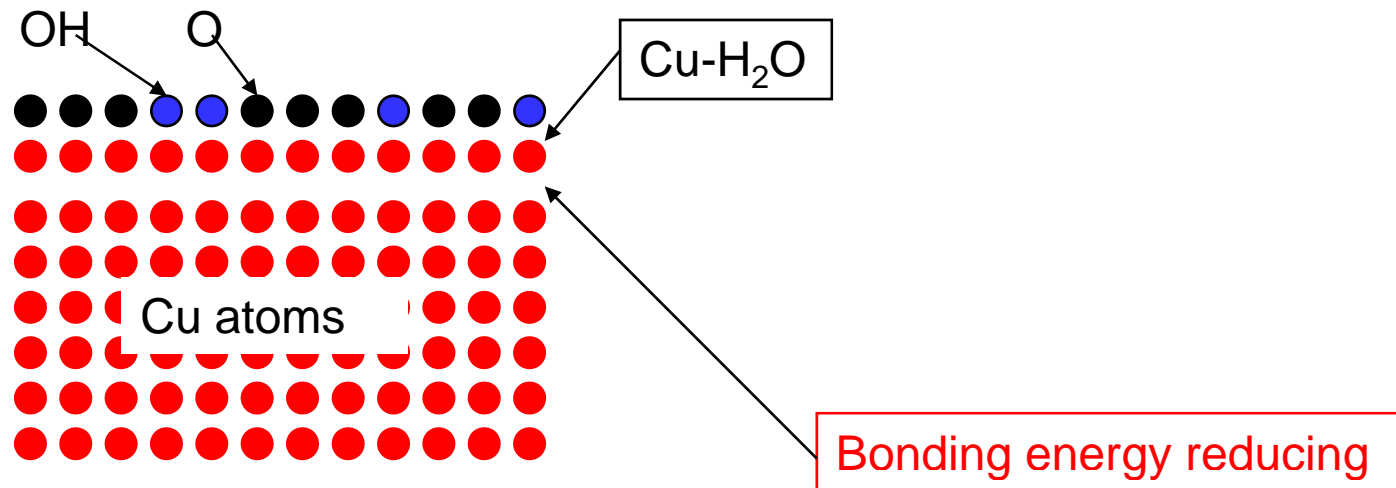
CO₂



Comparison of oil cutting and oil-less cutting

Copper oxide surface

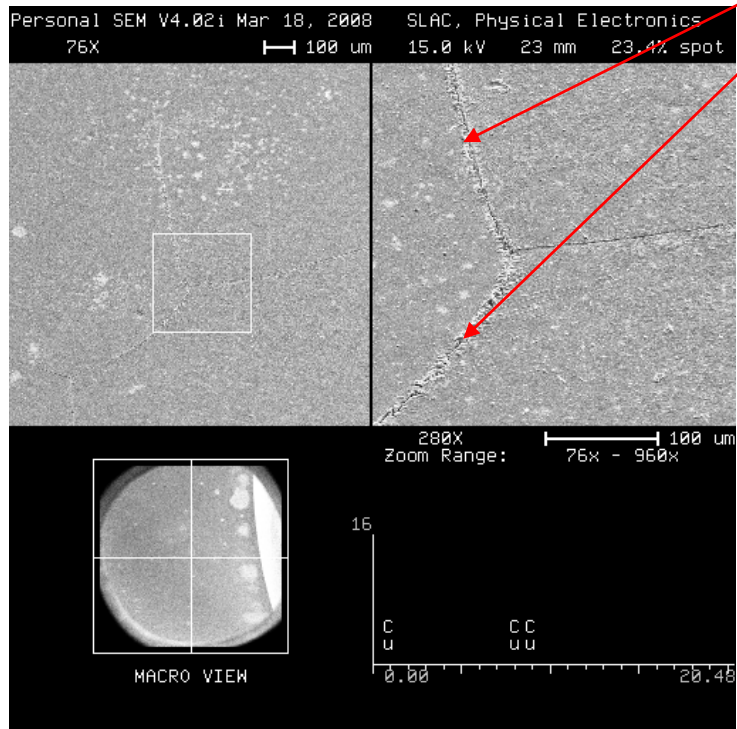
First principle molecular dynamics simulation
done by Osaka Uni.



CuO/Cu₂O layer easily evaporate by kinematics electron/ions ?

Grain size/boundary

Reducing breakdown rate on grain boundaries

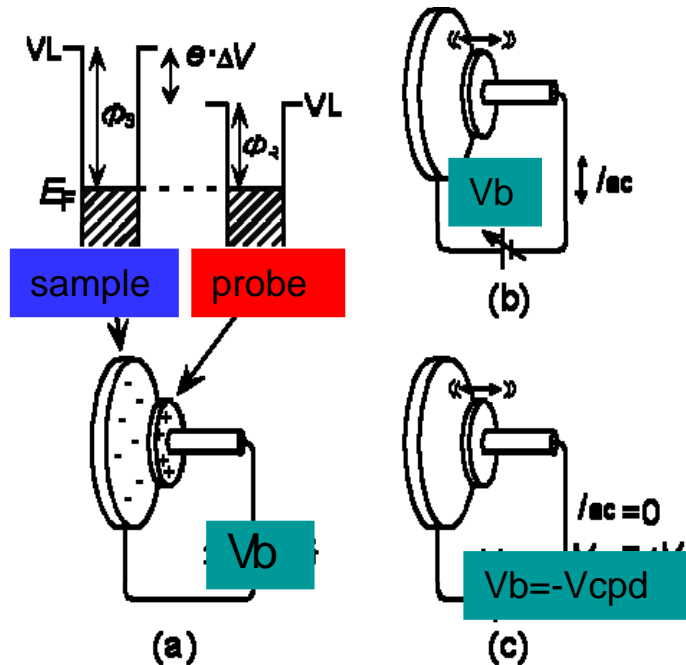


6N



6N/HIP

Work function measurement using Kelvin techniques

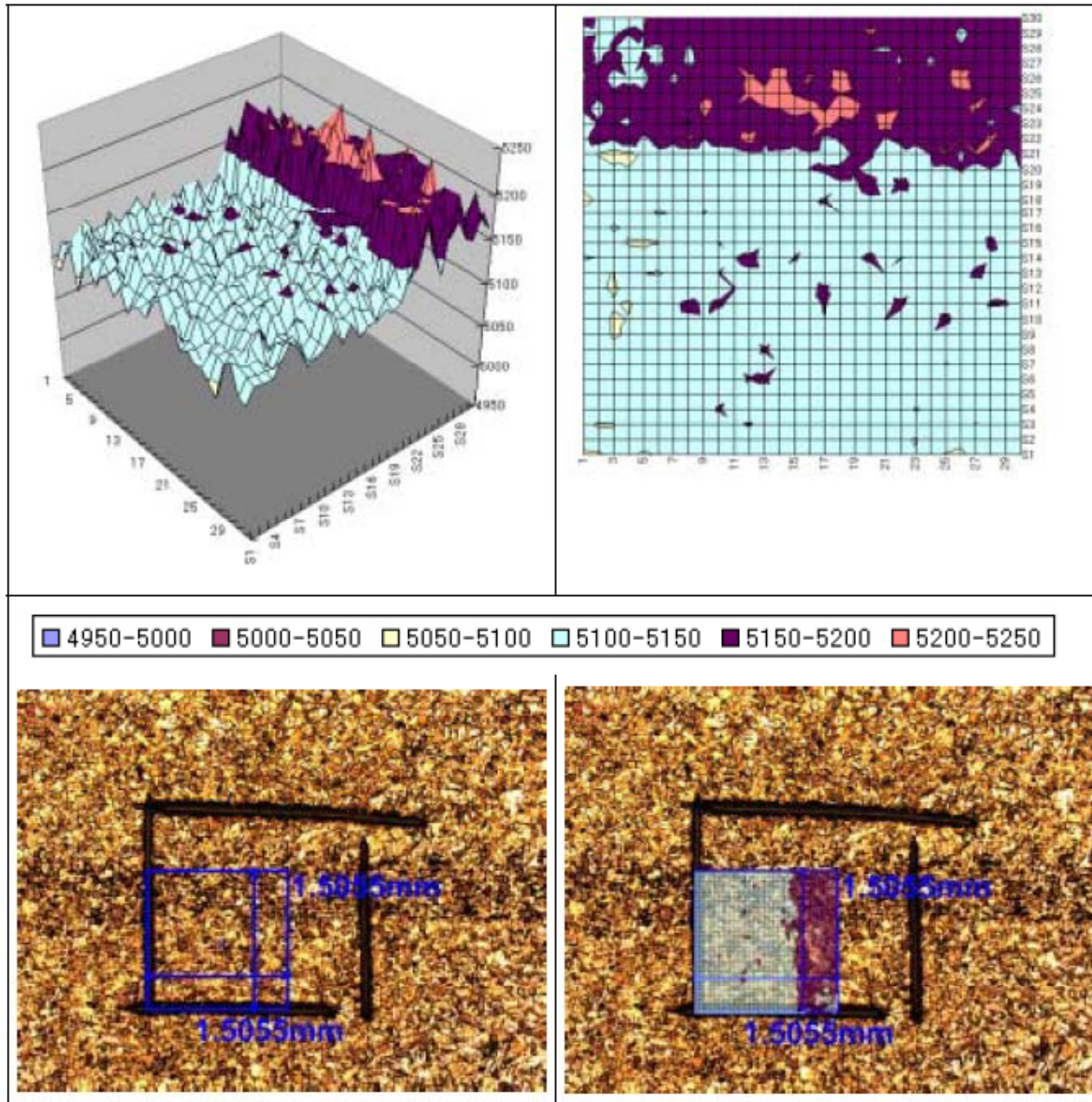


Measuring conditions

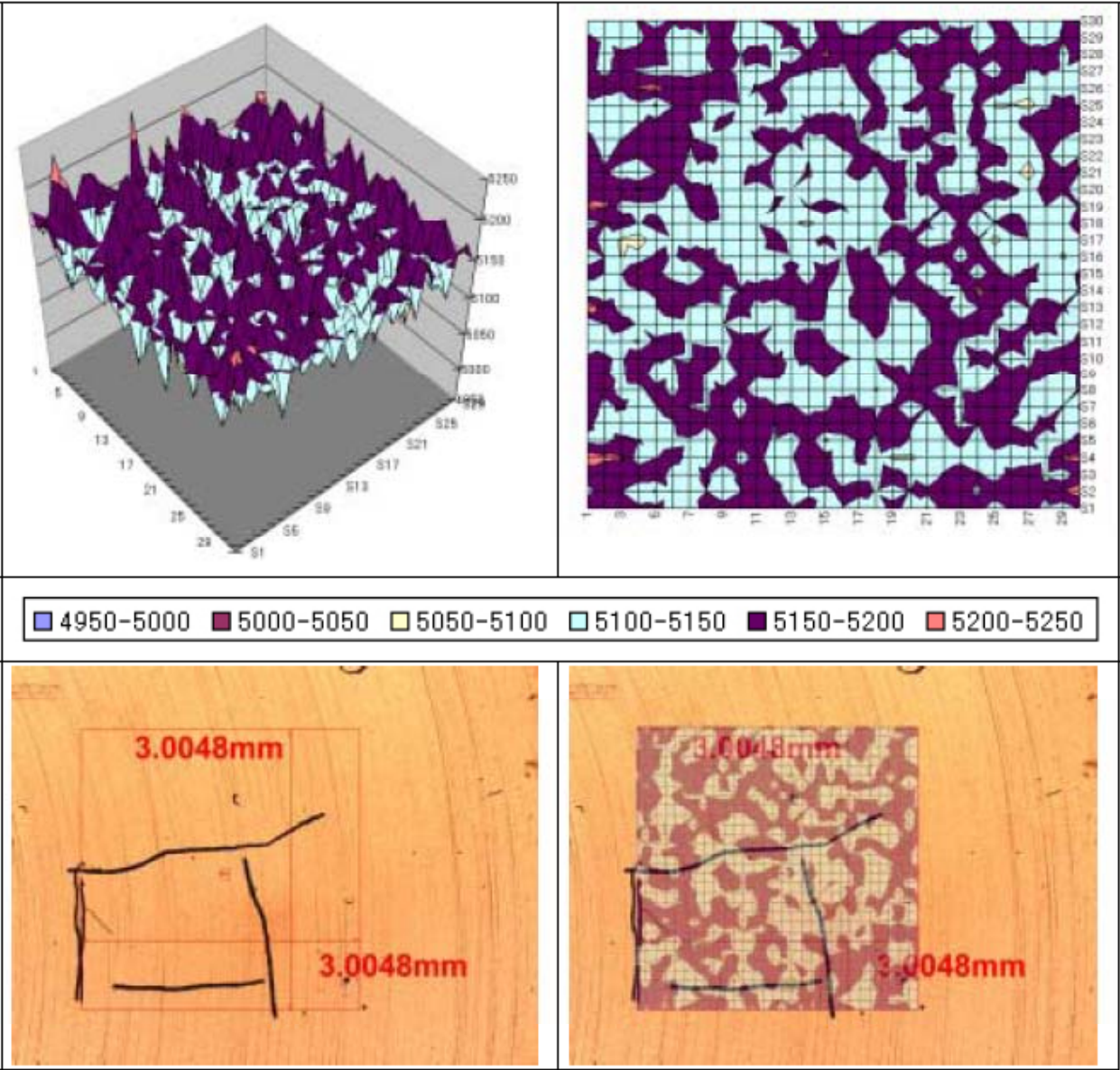
-Probe dia.	0.3mm ϕ
-Material /WF	Au /5.28eV
-Scanning	100 μ m pitch
-Area	3mmx3mm
Sample	including grain boundaries

The Kelvin Probe consists of a vibrating reference electrode in plane parallel orientation to the sample, creating a capacitor. The sample and probe are connected via a voltage source called the "backing potential" (V_b). When V_b is set to zero, a contact potential difference (V_{cpd}) equal to the *difference* in the probe and sample work functions appears across the probe/sample faces. The change in work functions is detectable because $wf = eV_{cpd}$ where e is the electronic charge. At the unique point where $V_b = -V_{cpd}$ the circuit is balanced, and the electric field between the plates vanishes resulting in a null output signal. This null condition, and deviations from it, can be detected with high precision, thereby directly measuring the changing sample work function.

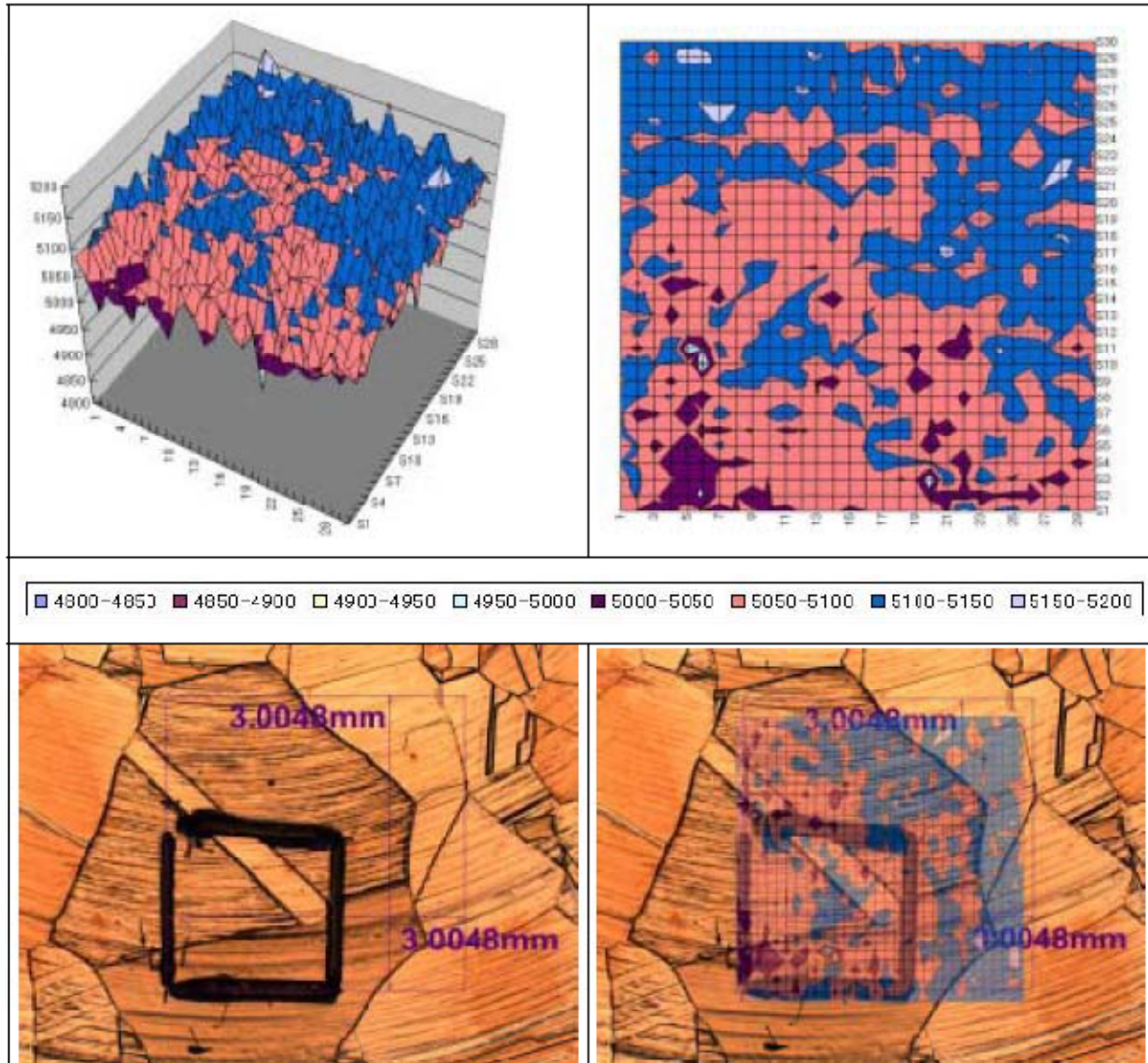
Class 1 sample



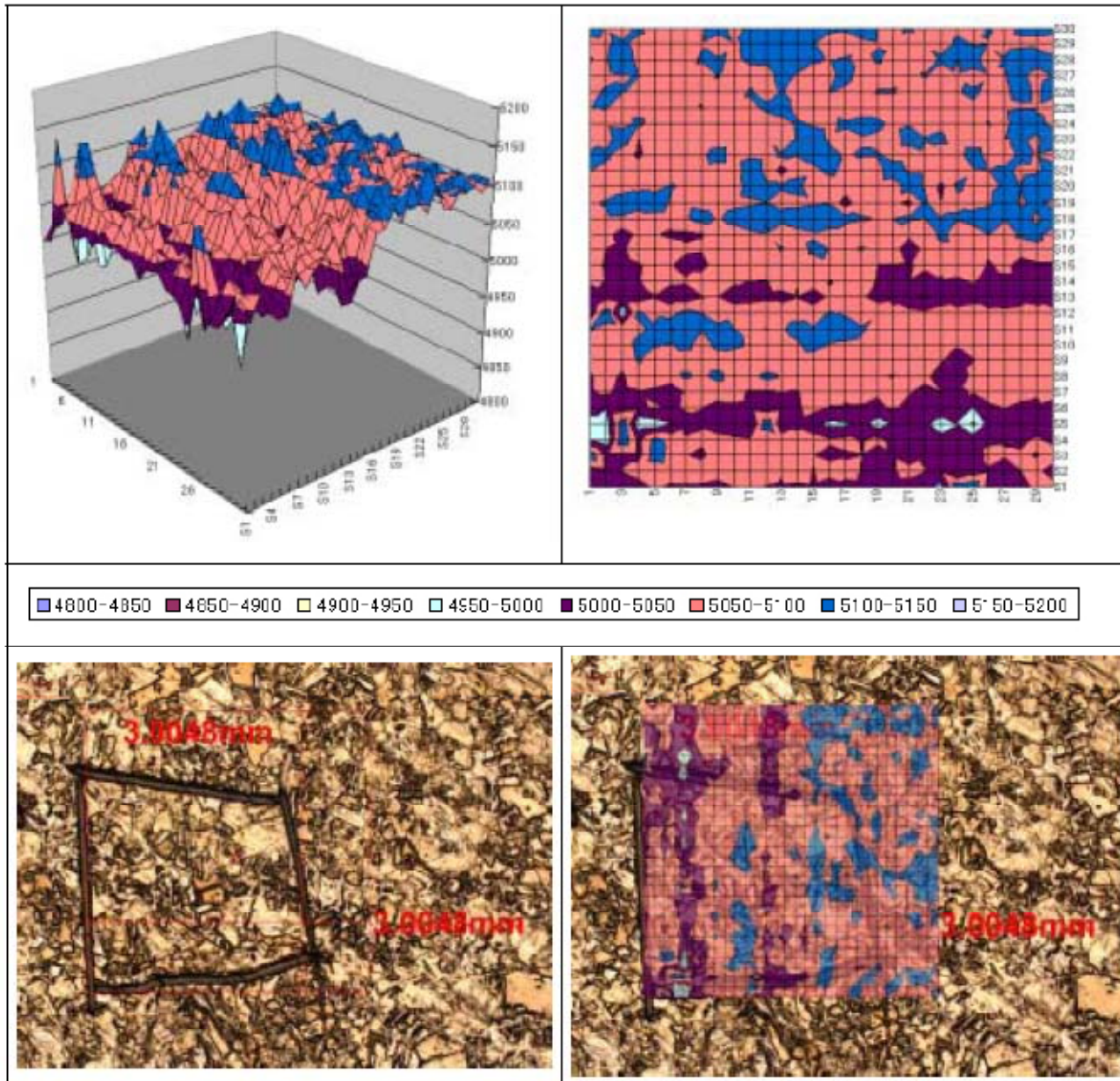
CuZr sample



6N/HIP copper sample



6N copper sample



Calculation of field emission current at 200MV/m using measured work function

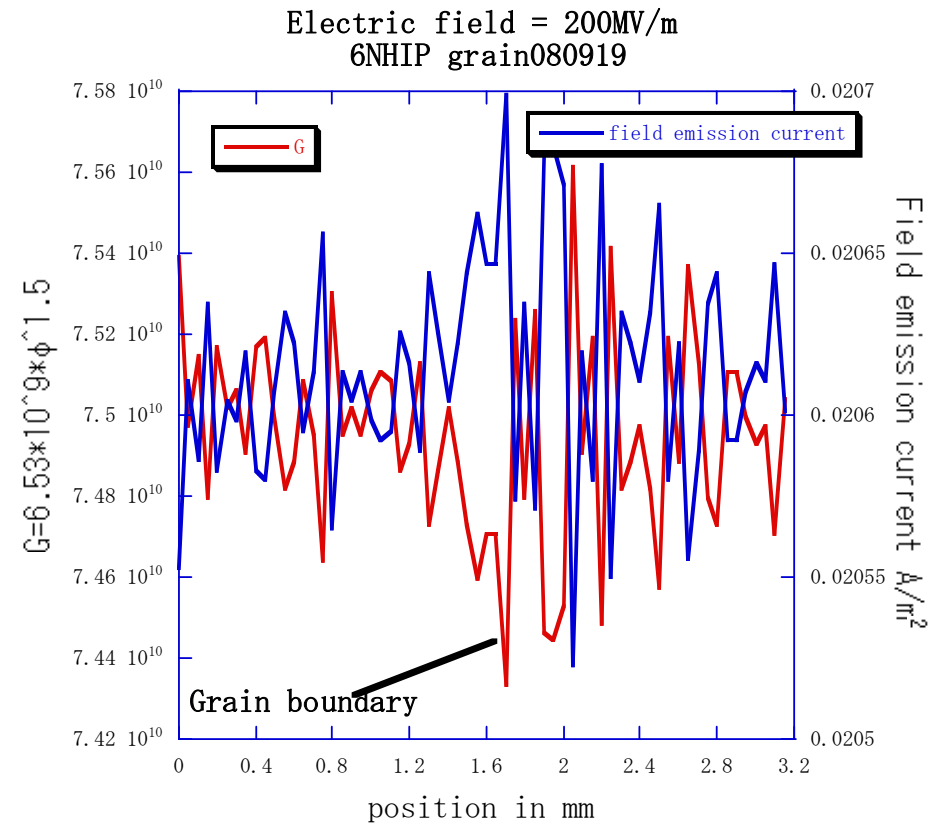
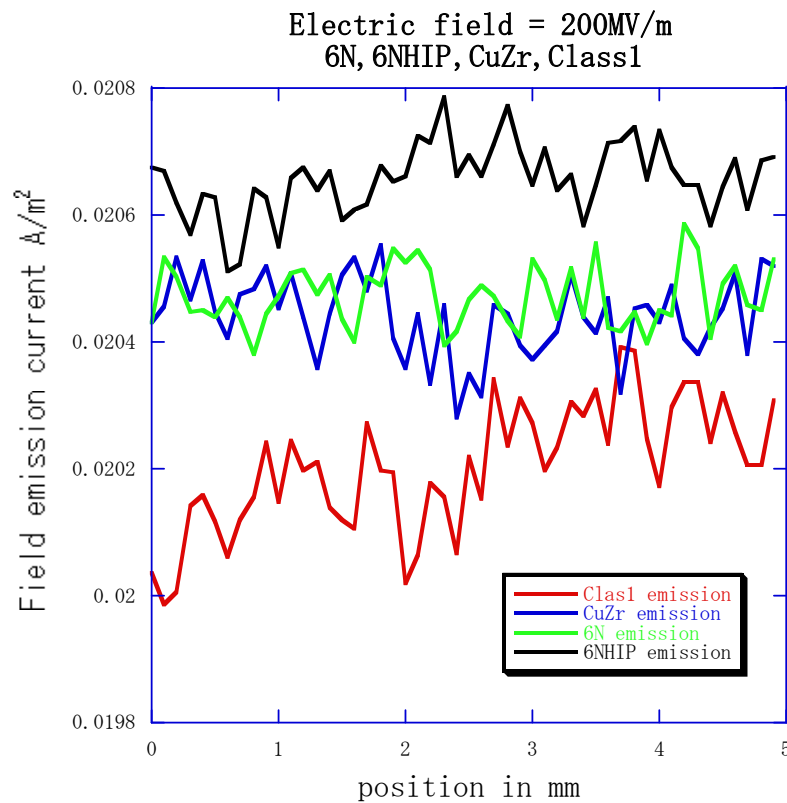
Purpose

Measurement of field emission enhancement at grain boundary

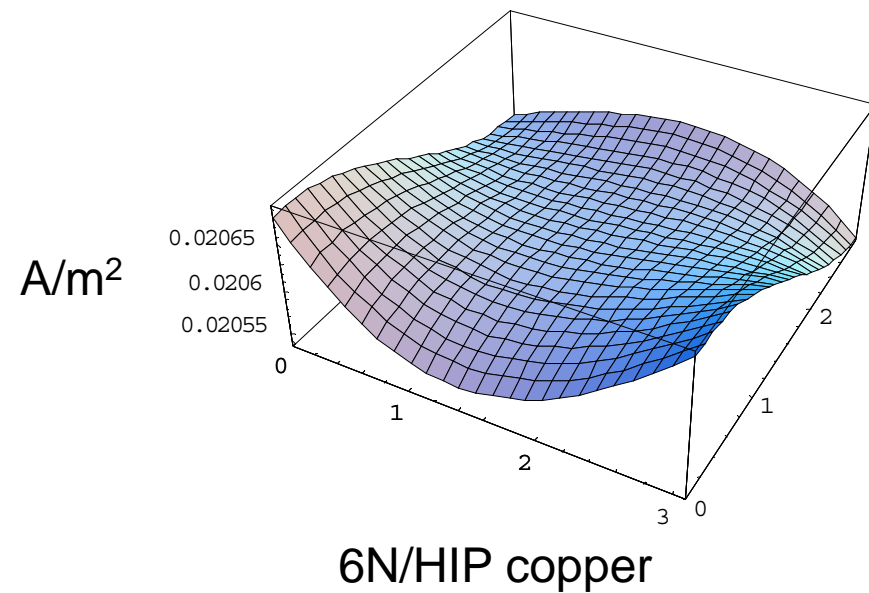
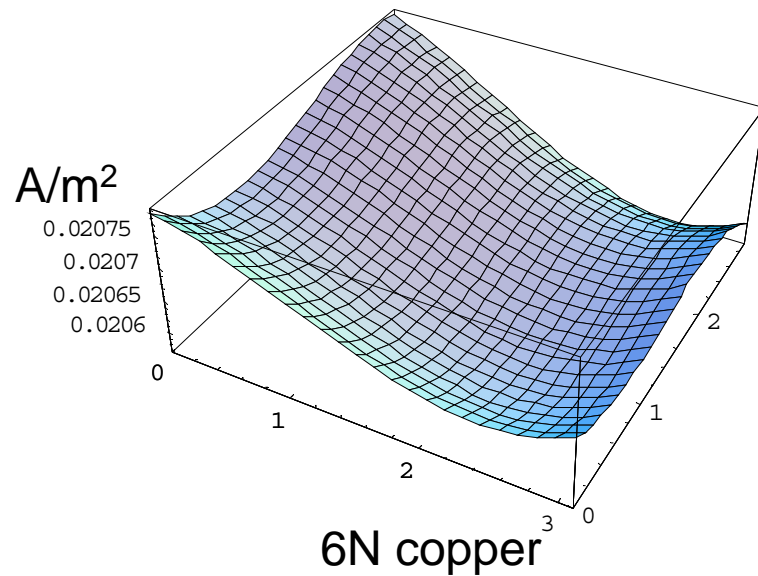
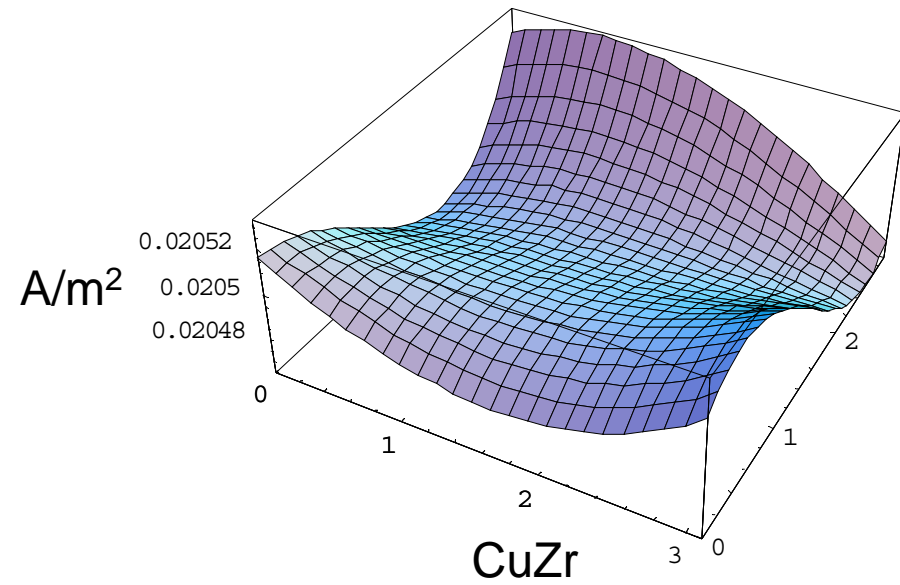
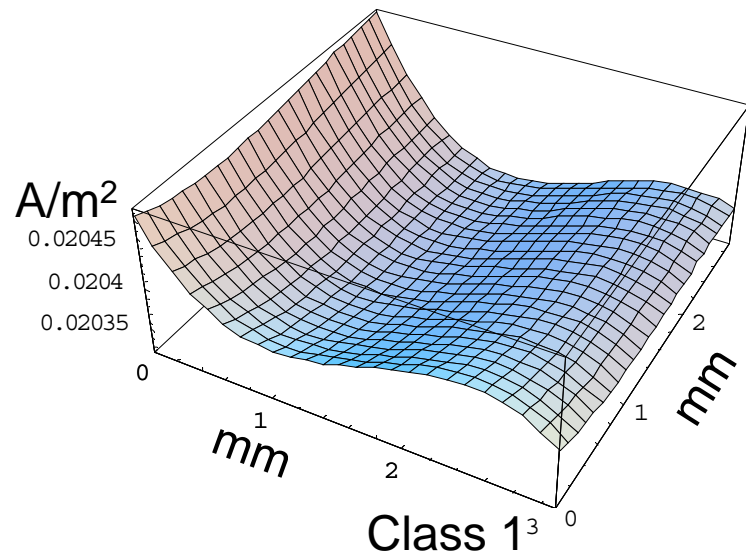
Work function measurement

Method : Kelvin method

Probe: 0.3mm ϕ , Environment: in air



Field emission at 200MV/m with $\beta = 1$



Results

@ All samples Work function are similar

@ All samples Field emission are similar

→ Measuring sensitivity (lateral resolution)
was low!!

-
- Who decide β value ?

Attempt on small amount of dark current and breakdown late at high gradient by removing particles and metal impurities on the cavity surface

removing particles and metal impurities techniques

- **Using a semiconductor wet cleaning solution and Mega-sonic**

Making thin Cu₂O layer on the cavity surface

- **Vacuum baking at 500 deg.C**

Keeping good cleanness at installation into the high gradient test setup

- **Making class 100 environment**

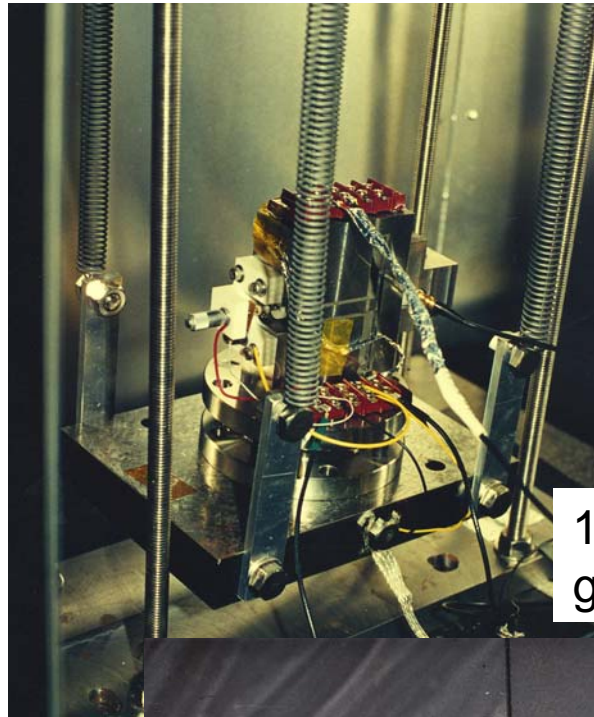
High gradient test structures

- **Single and 3-cell SW structure**

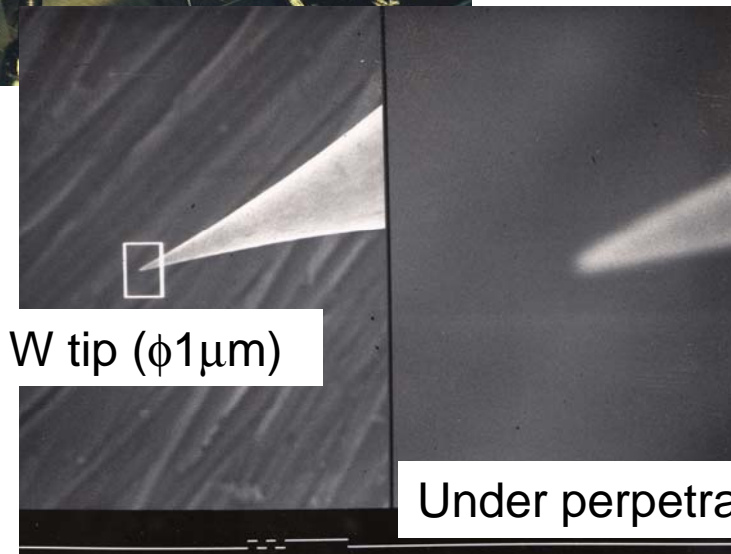
Test data analysis

- **Needs statistically analysis**
- **Single cell : 7 structures, 3-cell : 5 structures should be required**

Scanning field emission microscopy



1~10 μ m
gap/100~1kV



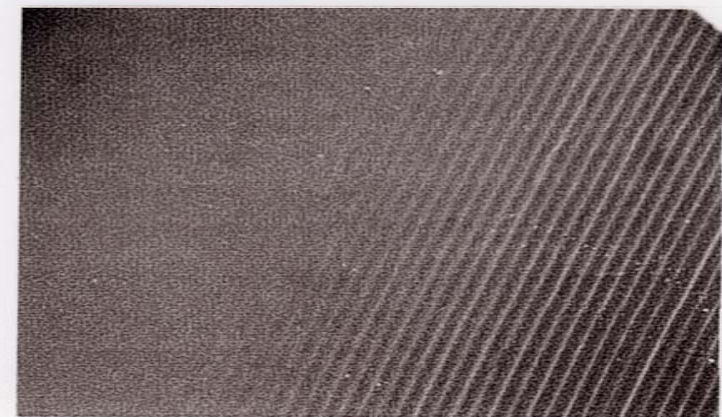
D.T surface

Ry 20nm

CMP Ry
1nm

Scanning

× 50



× 200

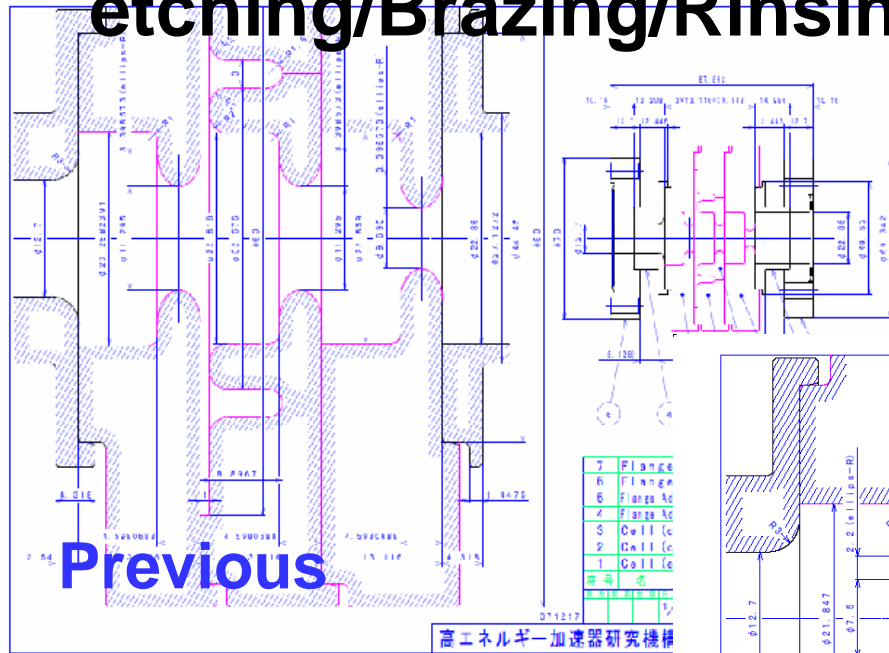
Future plan

- New choke structure fabrication
(1C-SW-A3.65-T2.6-Ellips-R2.2-CH 4.0)
using **6N/HIP**, **CuZr** and **CuAg** material.
- Comparison of the breakdown characteristics of Single cell SW structure
(1C-SW-A3.65-T2.6-Mf-KEK-#2)
using **Class1**, **6N**, **6N/HIP**, **CuZr**, **CuAg**
with advance technologies

(1C-SW-A3.65-T2.6-Ellips-R2.2-CH 4.0)

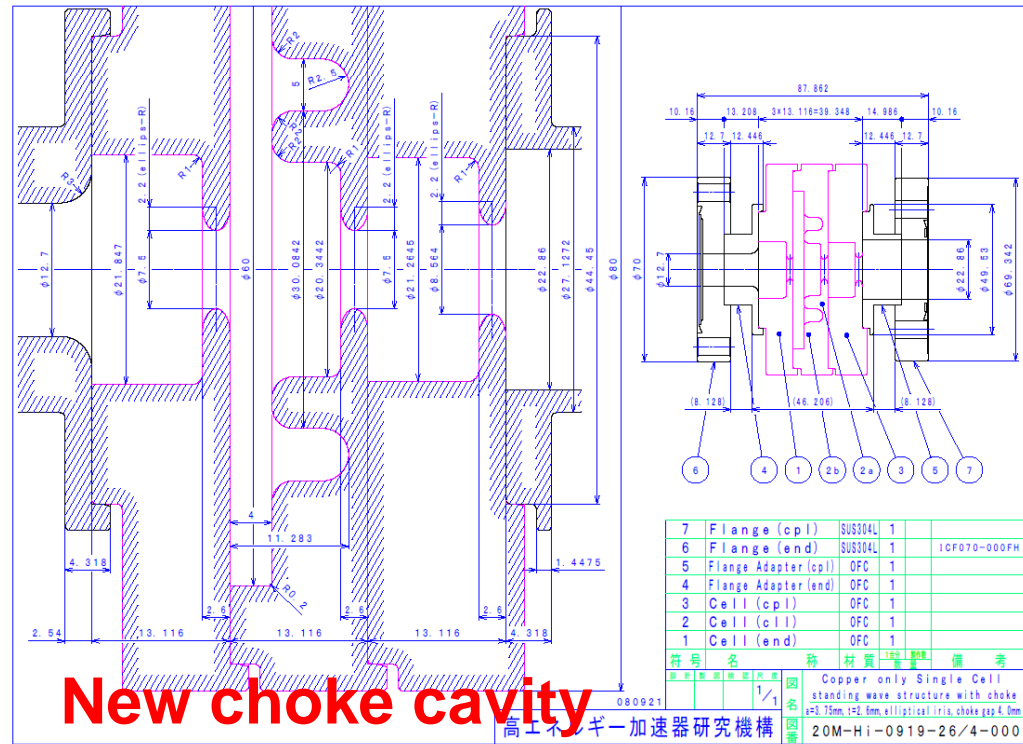
Diamond Tuning/ SLAC

etching/Brazing/Rinsing/Baking at 500degC.



Previous

RF designed by V. Dolgashev



New choke cavity

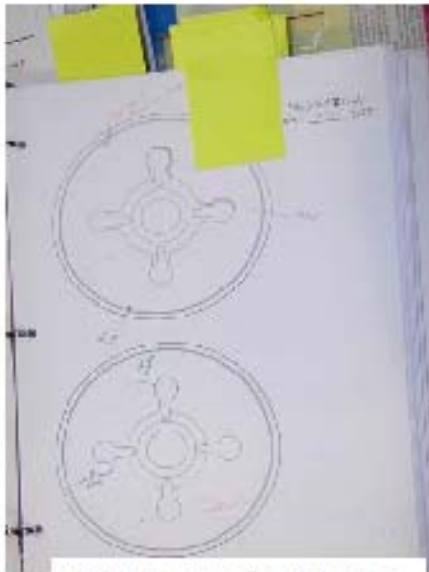
Schedule

- All structures will be fabricated by the end of December.

Future studies of cost effective
mass production

Construction of 60 cm NLC R&D Structures at SLAC

Bonding Operation
Two People
2.5 Hours Each



Cell Inspection Notes



Drawing



Traveller

First Assemble These:



Cells Just Cleaned

The Cell Inspection Notes Indicate Every Defect Pre-Cleaning. An Observation of Any "New" Defect Stops the Assembly Process.



Fixturing – Stainless Steel and Ceramics



While the Furnace is Set Up And Levelled;



A Dust Count is Taken; In This Case, Class 10,000.



The Cells Come from Cleaning in A Protective Box That is Taped Shut.



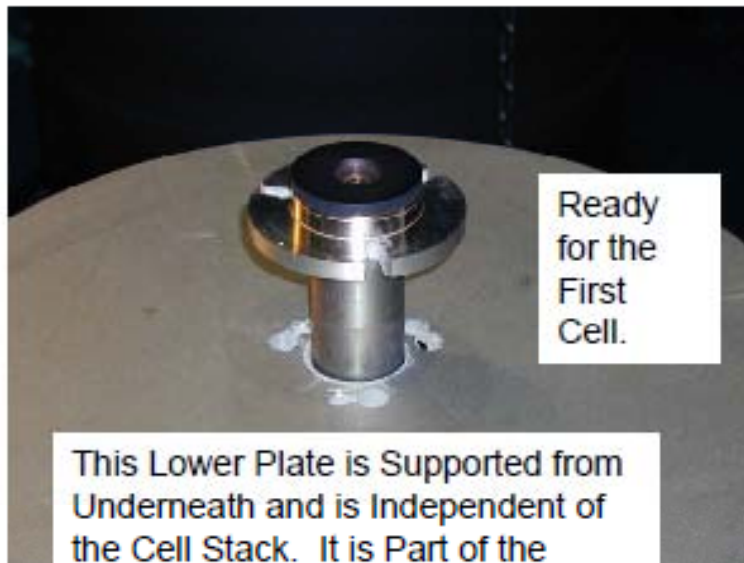
The Surveyor's Transit Used For Alignment Is Also Set-Up.



This Precise Surface is Part of the Fixturing, and the Copper Cells Will Bond to It.



A Flat Graphite Washer Will Prevent Any Adherence.



Ready for the First Cell.

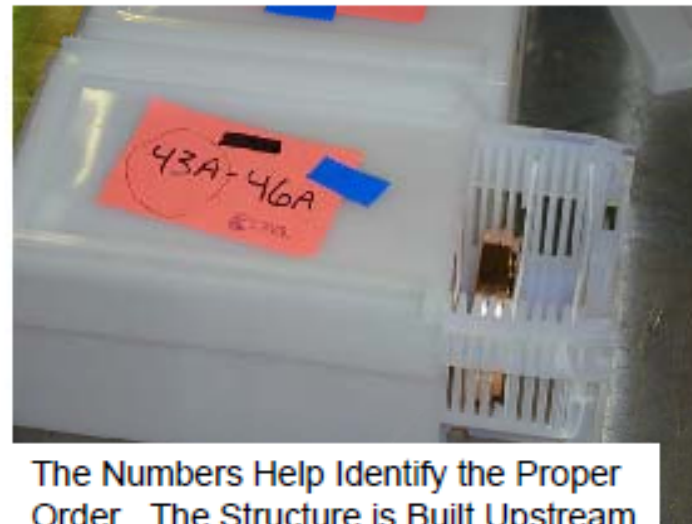
This Lower Plate is Supported from Underneath and is Independent of the Cell Stack. It is Part of the Weight System During Bonding.



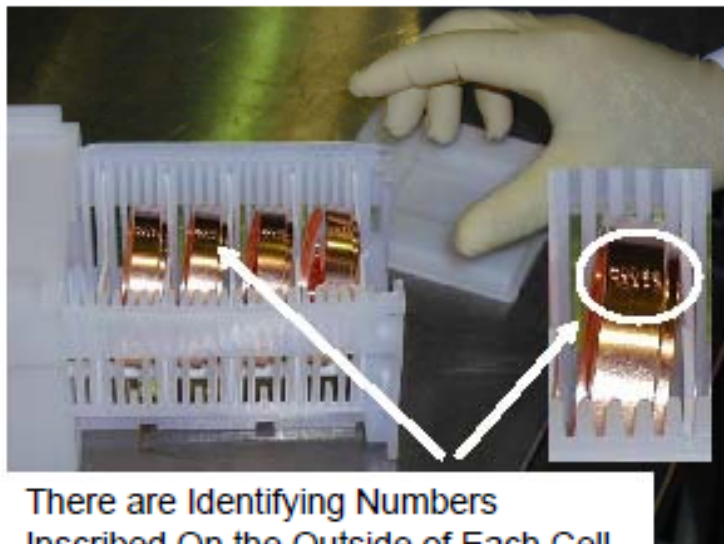
The Graphite is Carefully Aligned.



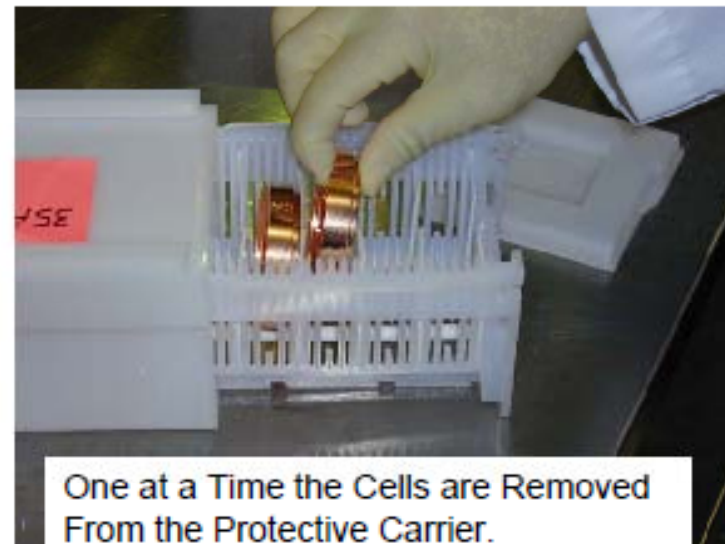
The Clean Boxes with Cells are Lined Up in Order on a Cart.



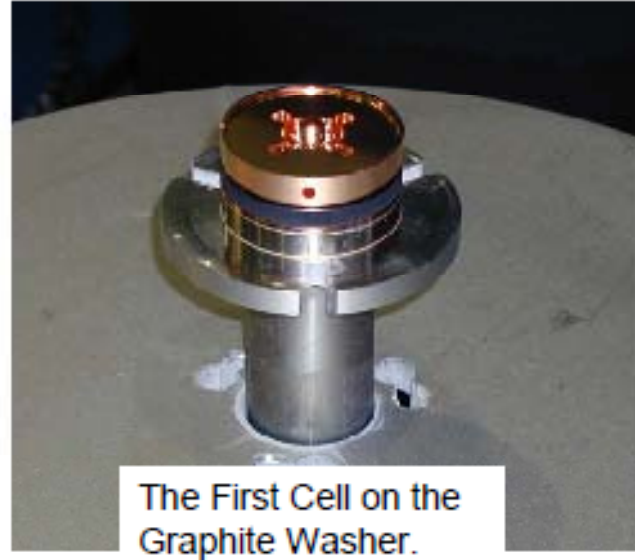
The Numbers Help Identify the Proper Order. The Structure is Built Upstream End Up.



There are Identifying Numbers Inscribed On the Outside of Each Cell.



One at a Time the Cells are Removed From the Protective Carrier.

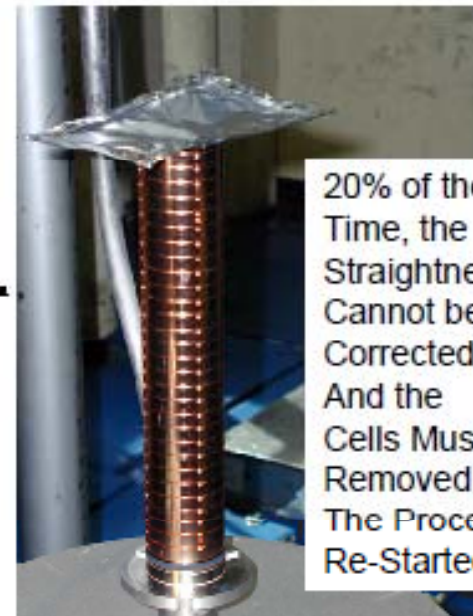
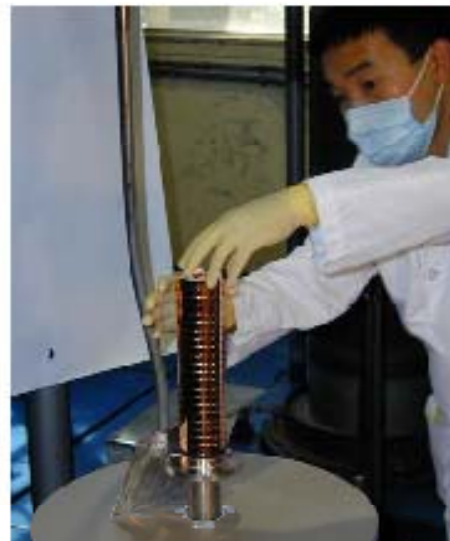




Both Rotational and Vertical Alignment are Checked to the Limits of the Transit – a Few Mils.



As a Result, Very Fine Adjustments are Made for Almost Every Cell Assembled.



20% of the Time, the Straightness Cannot be Corrected, And the Cells Must be Removed and The Process Re-Started.

Note the Clean-Room Attire – Coats, Gloves, Masks

Since the Cells Nest Into Each Other, They Must Be Assembled Parallel To the Next Cell.



The Technician With the Transit then Directs Tiny Alignment Changes. Alignment Takes Up Most of the Total Time Required.



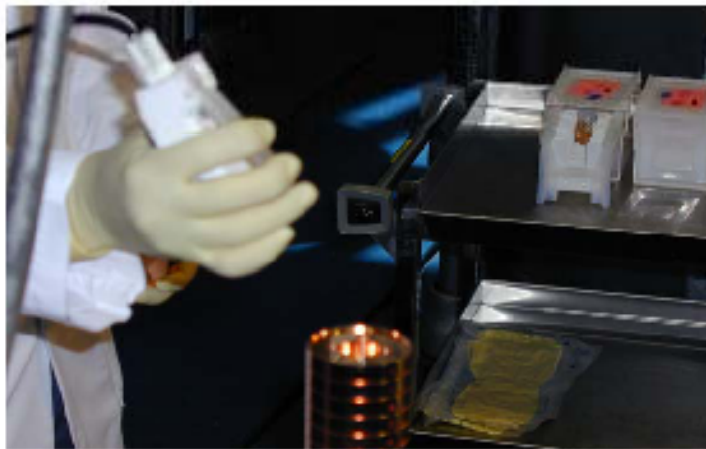
Sometimes Even the Physicist is Notified.

Each Cell is Inspected Before Assembly. Any Problems, Especially Those Not Noted in the Master Inspection Log, are Investigated.

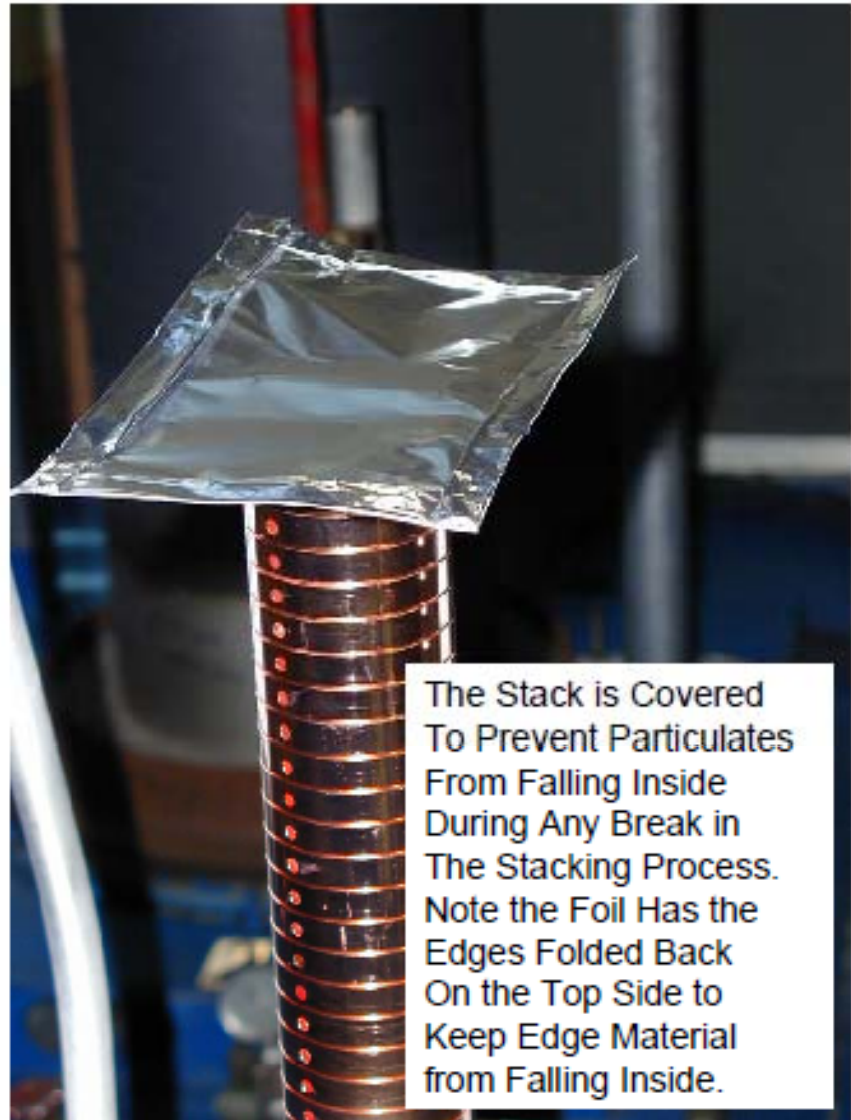


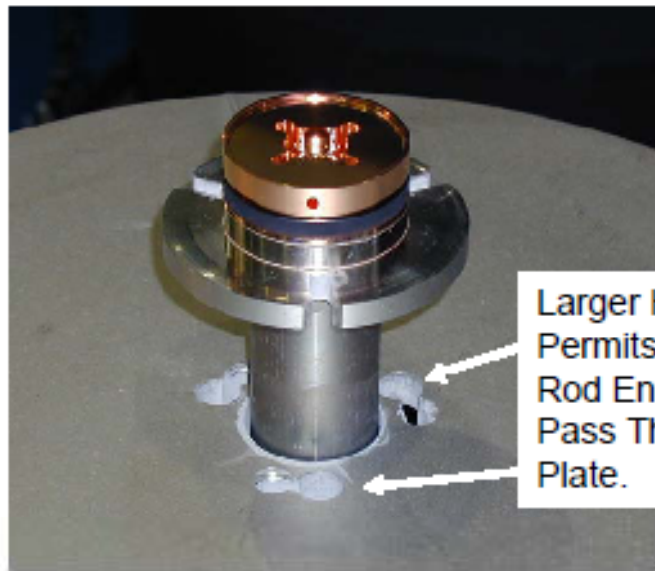
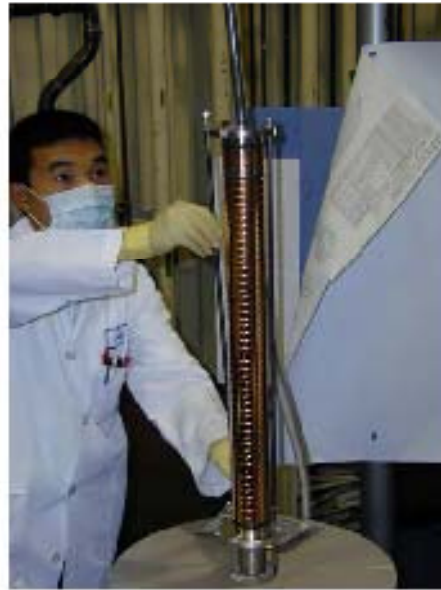
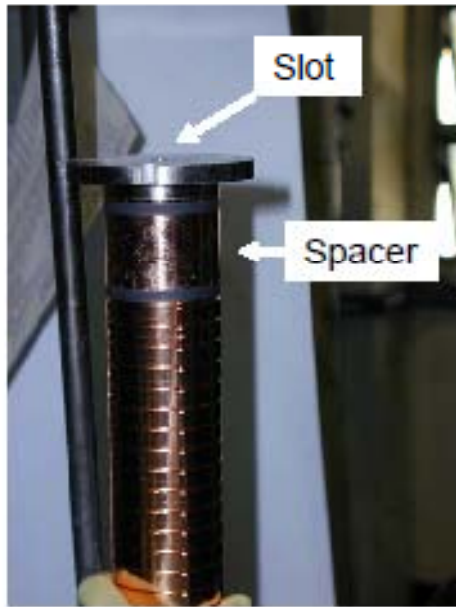


Sometimes Pressurized Filtered Nitrogen Is Used to Remove Particulates from a Cell.



Sometimes Pressurized Filtered Nitrogen Is Used to Remove Particulates from the Stack.





The Completed Stack Has More Graphite Washers and a Copper Spacer to Prevent Sticking and Reach the Length That Matches the Fixturing. Three Inconel Rods With Nuts are Then Added – They Fit Into Slots in the Top Washer and Holes in the Lower Plate.





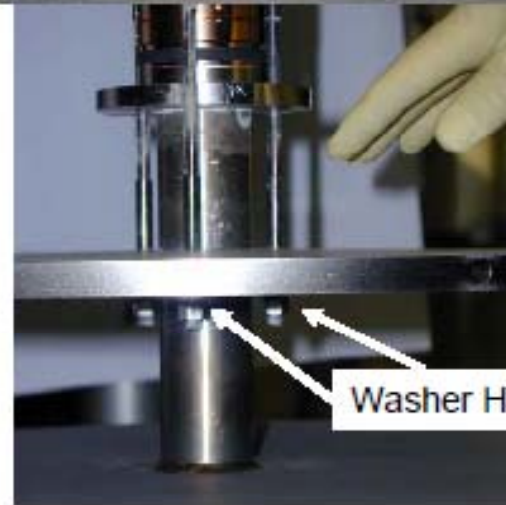
Once the Rods are Inserted, a Temporary Weight Prevents Shifting of the Cells.



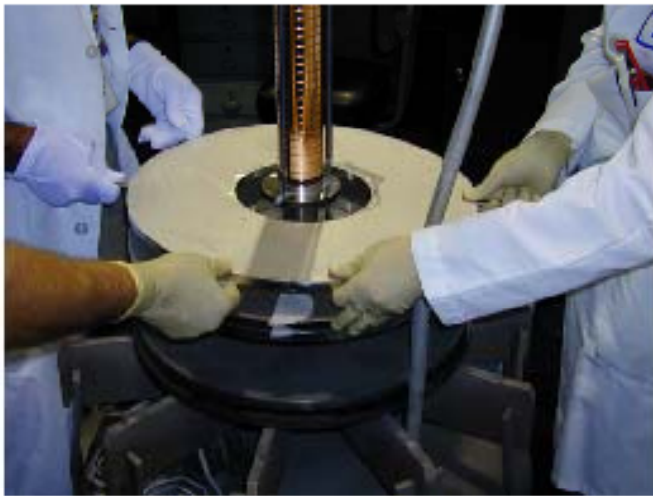
Supports for the Lower Plate are Carefully Removed. Its Weight is Then Transferred to the Top of the Structure Through the Three Rods.



Structure with One Plate.



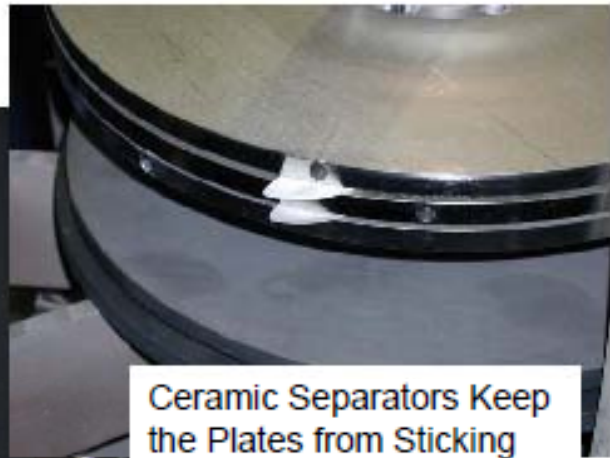
U-Shaped Washers Slide Between the Nuts and Plate on Each Rod to Lock the Plate on the Three Rods.



Two More Plates (Additional Weight) Must Go On.



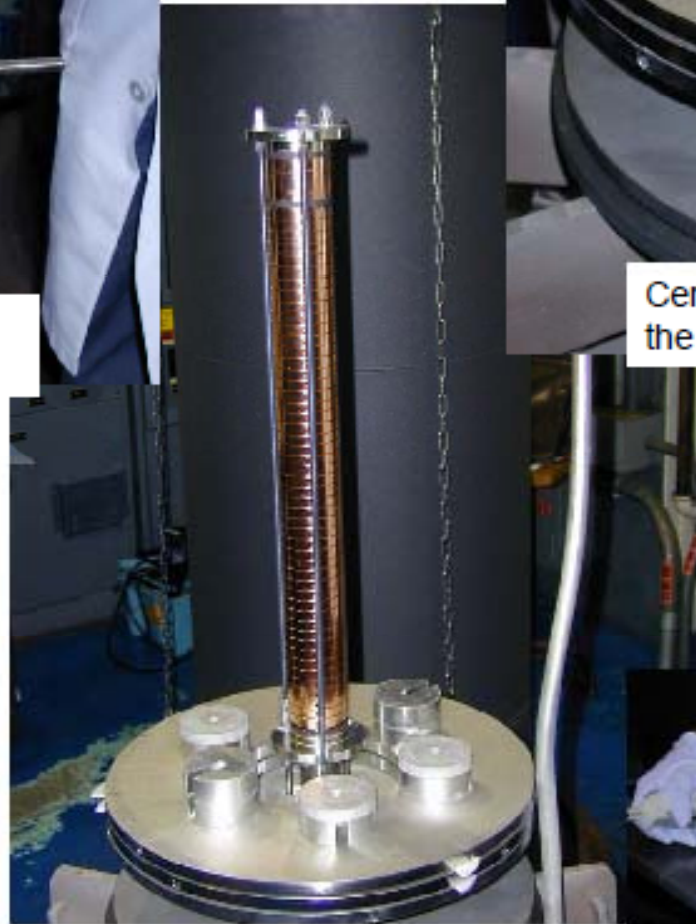
Rods in Holes Allow the Plates to be Handled.



Ceramic Separators Keep the Plates from Sticking



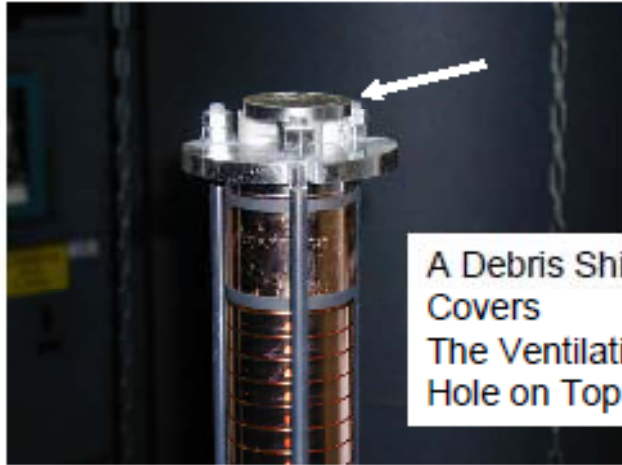
The Weight is Evenly Distributed.



Weight Application is Complete.



Smaller Weights are Blown Off with Nitrogen.



A Debris Shield
Covers
The Ventilation
Hole on Top.

Thermocouples
(Six) Are Added.



Ready for
Bonding.

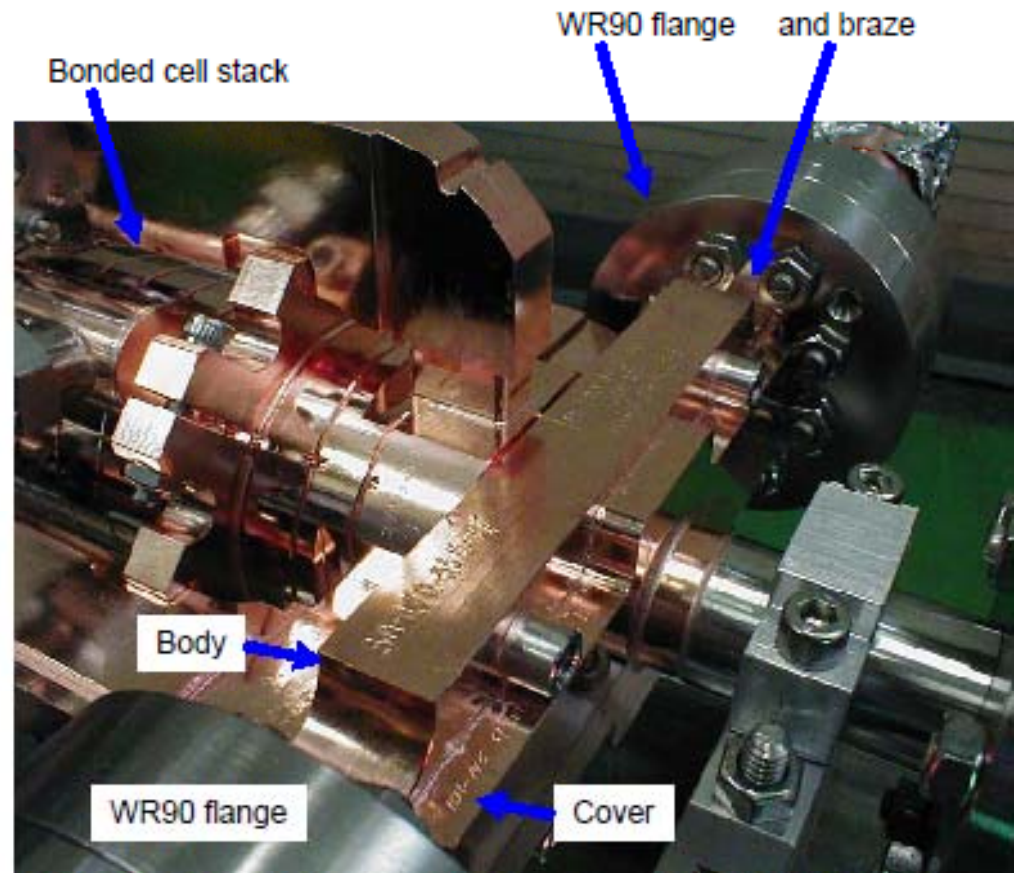
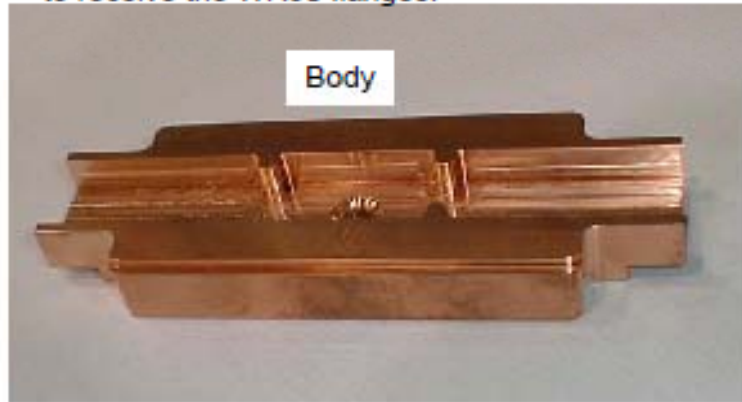


Go/No-Go Gauges Check the Disk
Spacing.

Building an NLC 60 cm Structure at SLAC

Excludes Bonding (See separate Bonding document)

The couplers are made by Robertson Precision and consist of a body and cover plate. They are brazed together and then the ends are machined to receive the WR90 flanges.



Once the flanges are on, a few of the cells are brazed to the coupler as well as the stainless steel cutoff tubing. It is then ready for brazing to the bonded cell assembly.



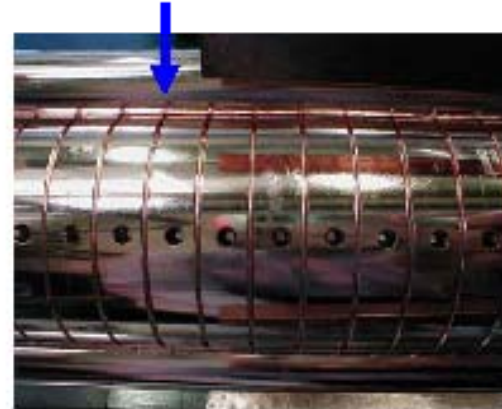
The couplers are brazed on in a standard retort hydrogen furnace in the Klystron building. The coupler being brazed is on the down side. This requires two braze steps. At the same time, the water cooling tubes are brazed on.

In this photo the wires holding the water tubes on for the final braze can be seen, as well as the fixturing for the coupler braze at the bottom.

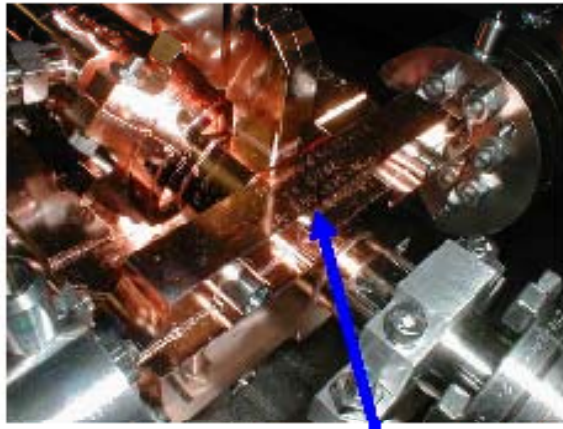


The structure here is dressed with the weights and thermocouples necessary to enable it to be properly brazed.

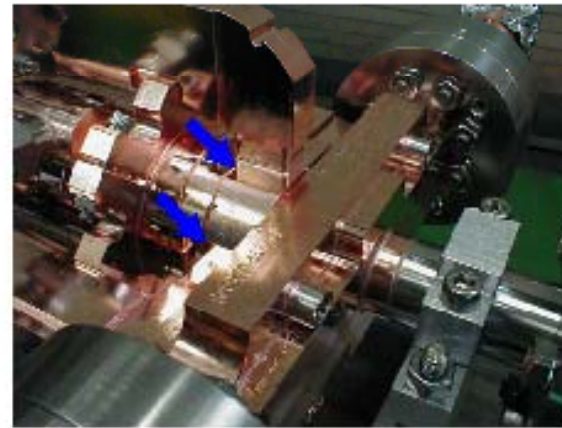
Braze alloy is also added into the area between cells to make sure that each cell to cell joint is Vacuum tight and mechanically strong.



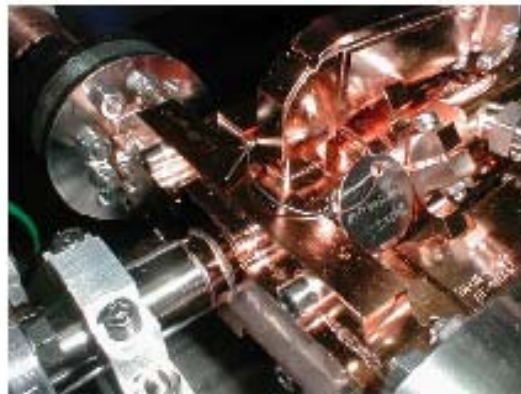
Tuning posts are brazed into each of the small holes in four places on each cell to enable them to be tuned up or down in frequency.



Piece part, subassembly, and final assembly information is stenciled into every respective part.



This structure has HOM waveguides included, four per end, eight total. They emerge from the cell just inboard of each fundamental coupler.

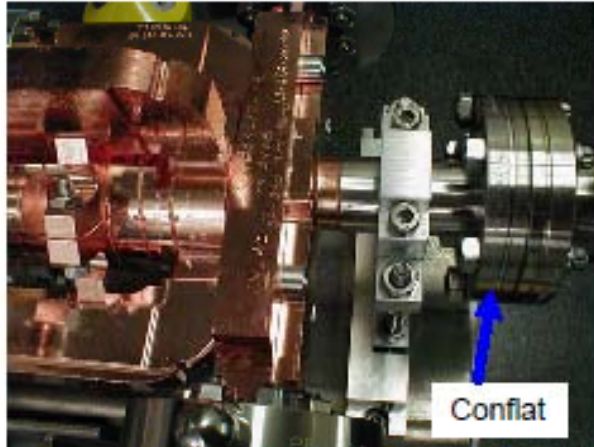


Metal I.D. tags are also used.

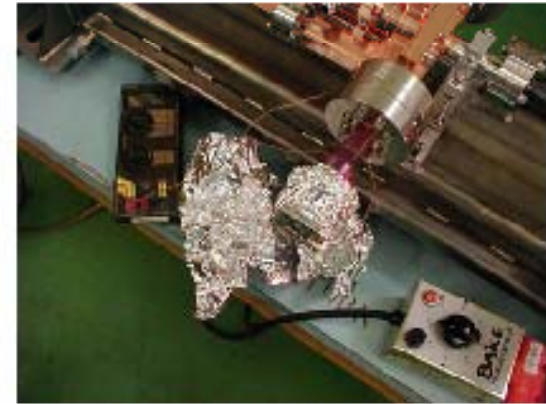


Water fitting for structure cooling

Part and serial number



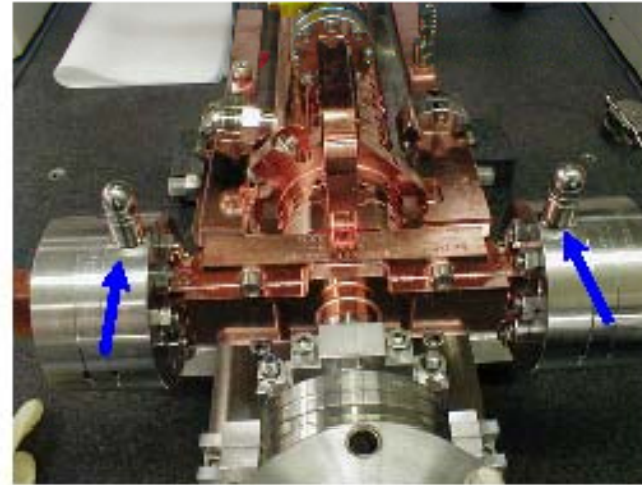
There are Conflat flanges put on both ends of the structure on the cut-off tubes. They used to be done prior to bakeout, but now they are done before bakeout so that we do not accidentally add contamination during the welding.



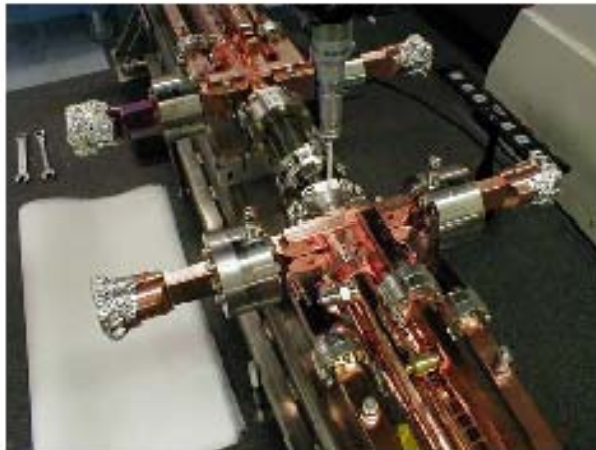
Adapter to change the flange sex.



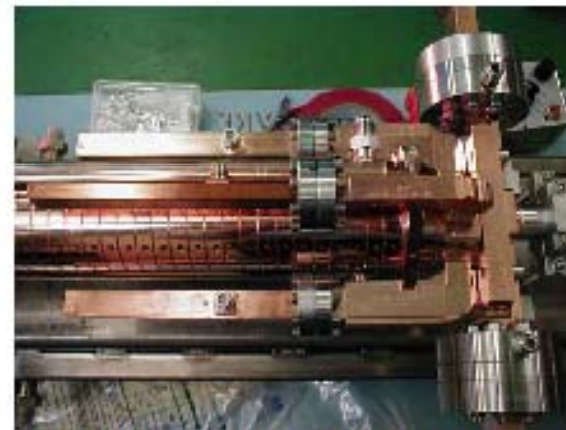
If a flange leaks it is baked out with heater tape, usually resulting in an NIL seal. The heated copper part gets discolored.



Tooling balls are added to help with the alignment in the tunnel (these structures are going to ASSET)

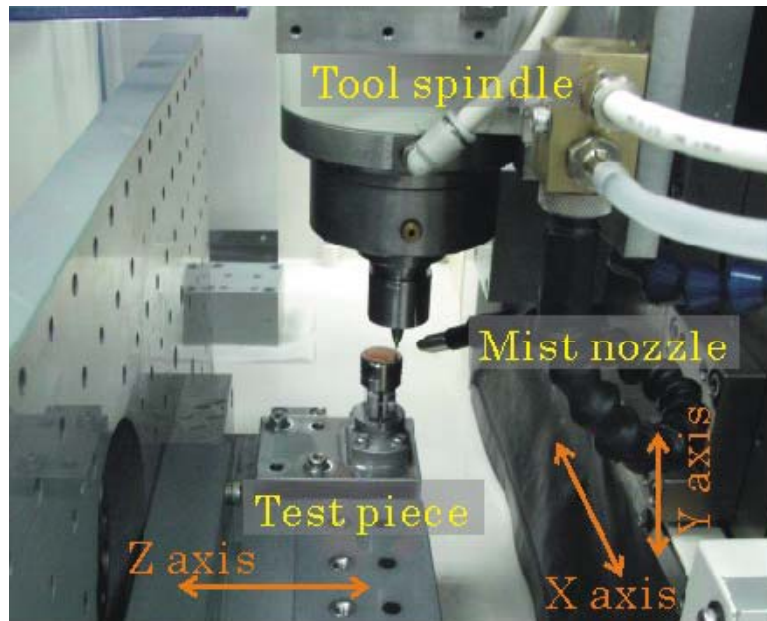


CMM measurements.



Since these structures are going to ASSET, there must be loads with monitoring on each HOM arm. These loads are made by CPI, are expensive, and will leak at the flanges or in the coax feed-through.

テストワークの加工結果

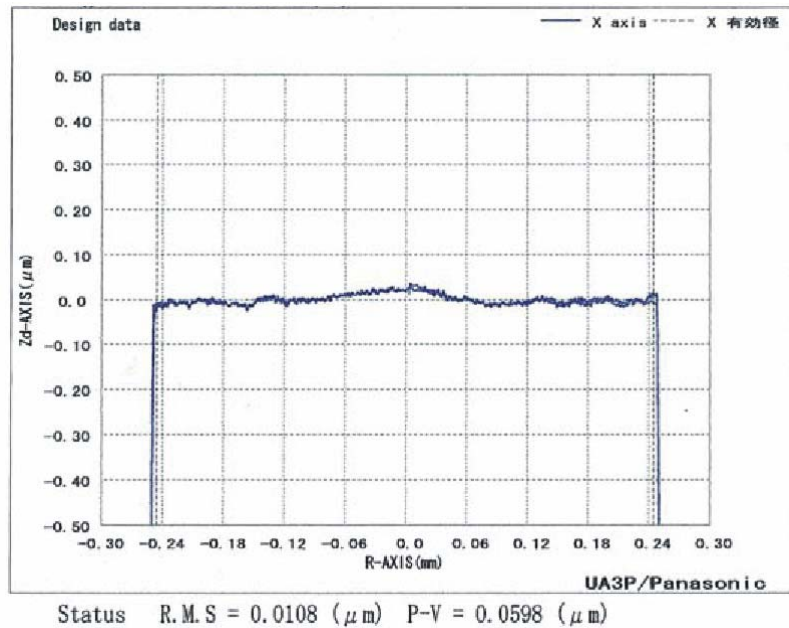


Cut setup for test piece
テストワーク加工の段取り

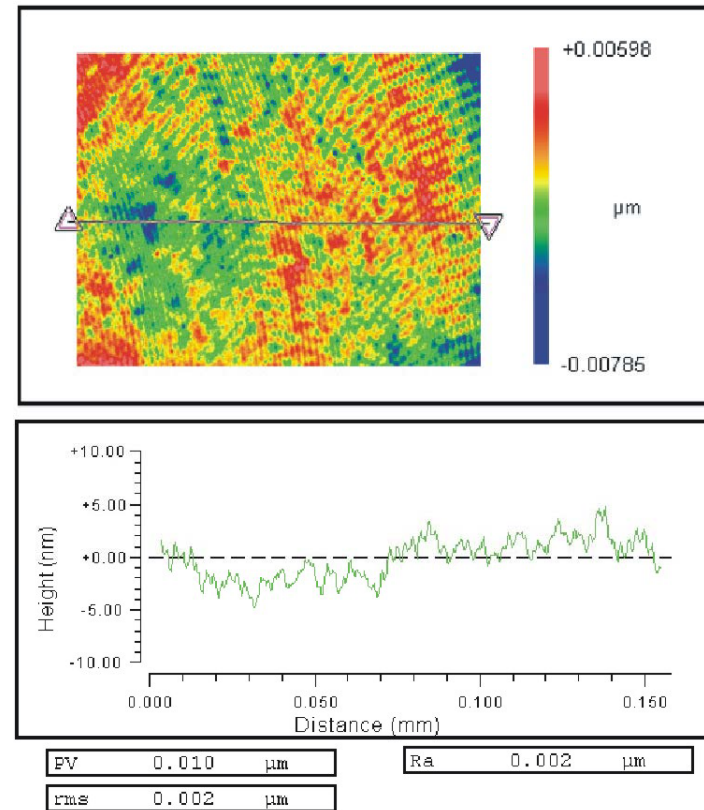


Cut surface of lens array
加工ワーク表面

テストワークの加工結果

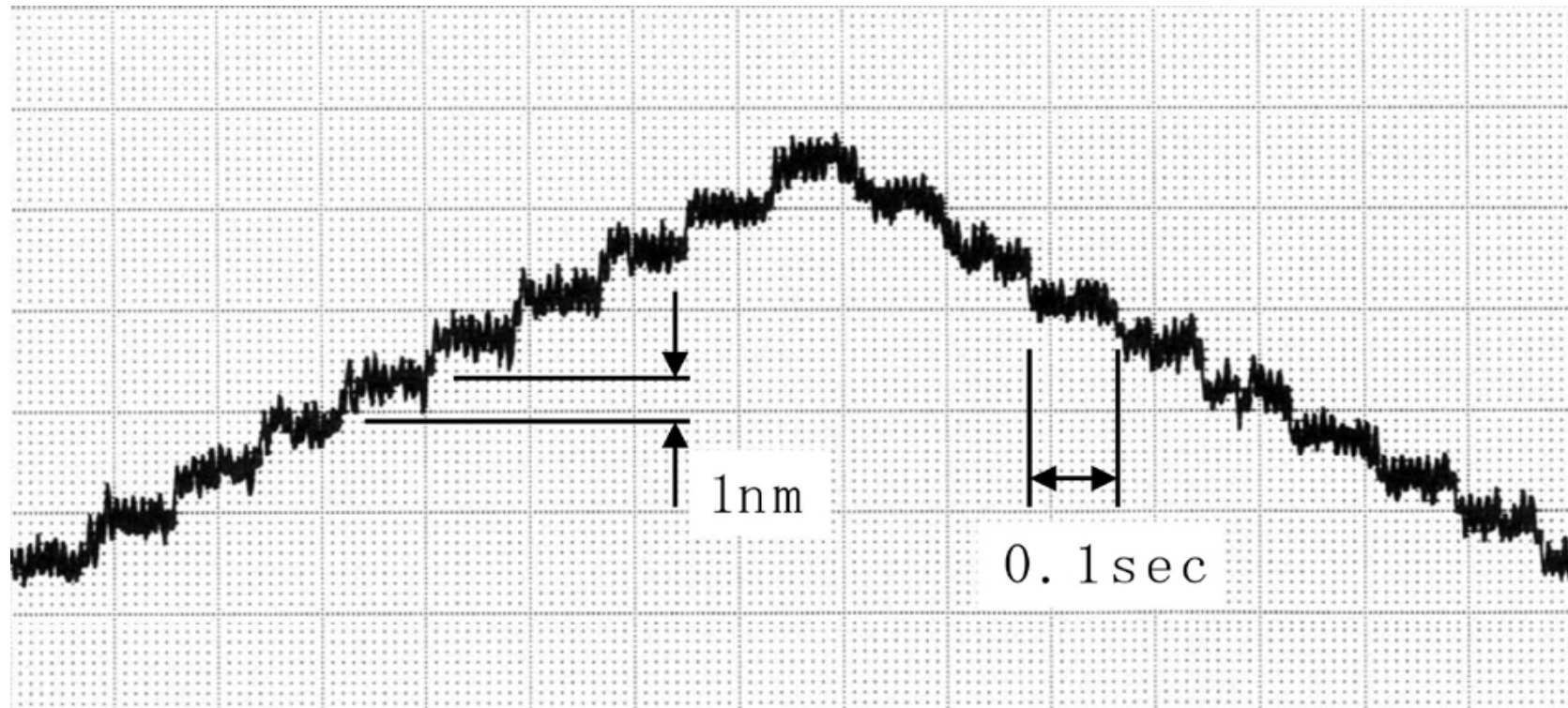


加工後の形状精度

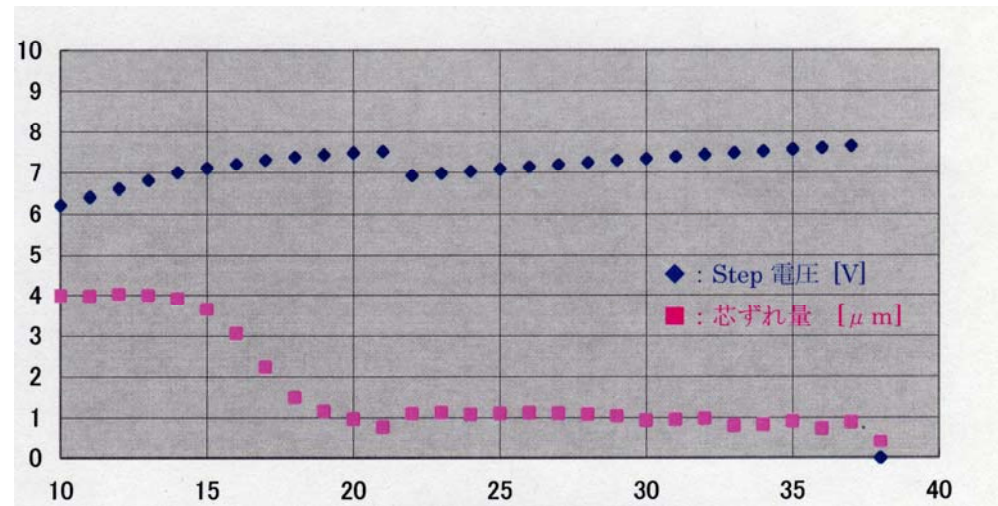
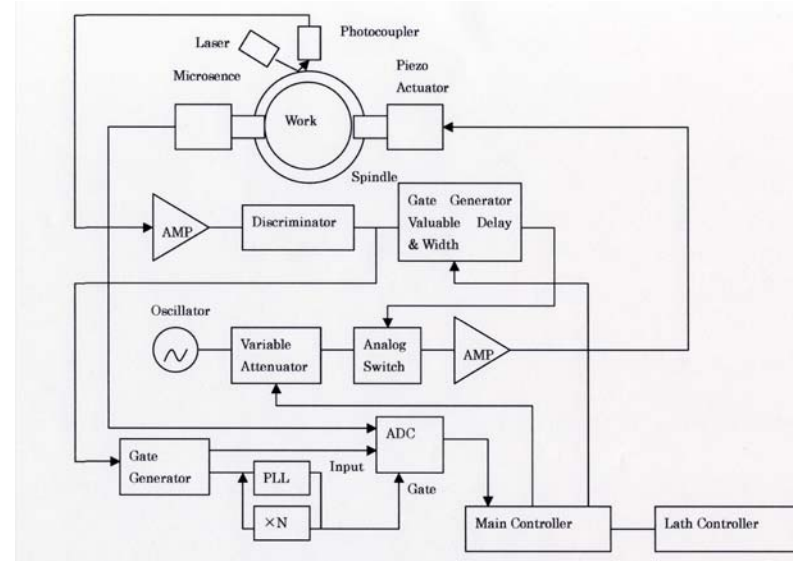
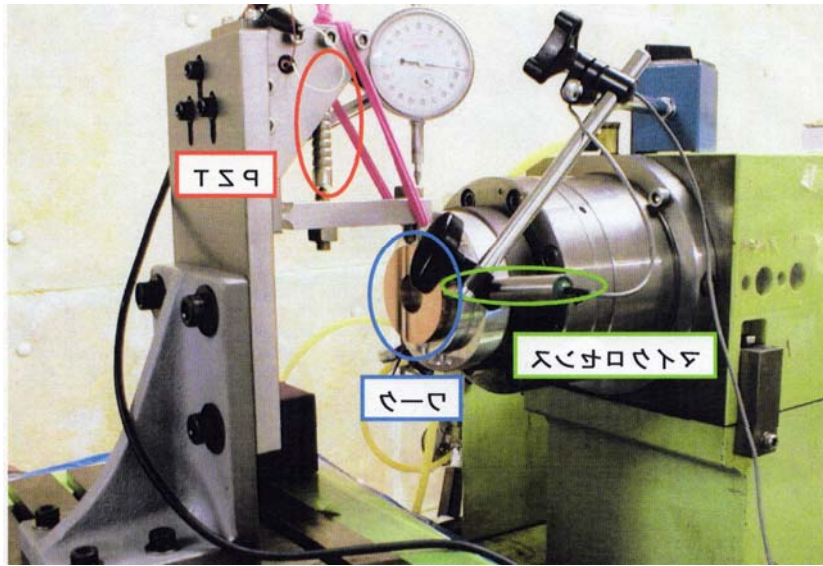


加工後の加工面性状





1nm step feed command response



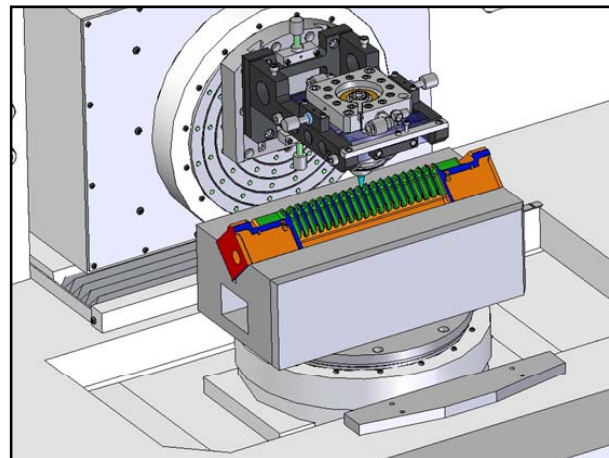
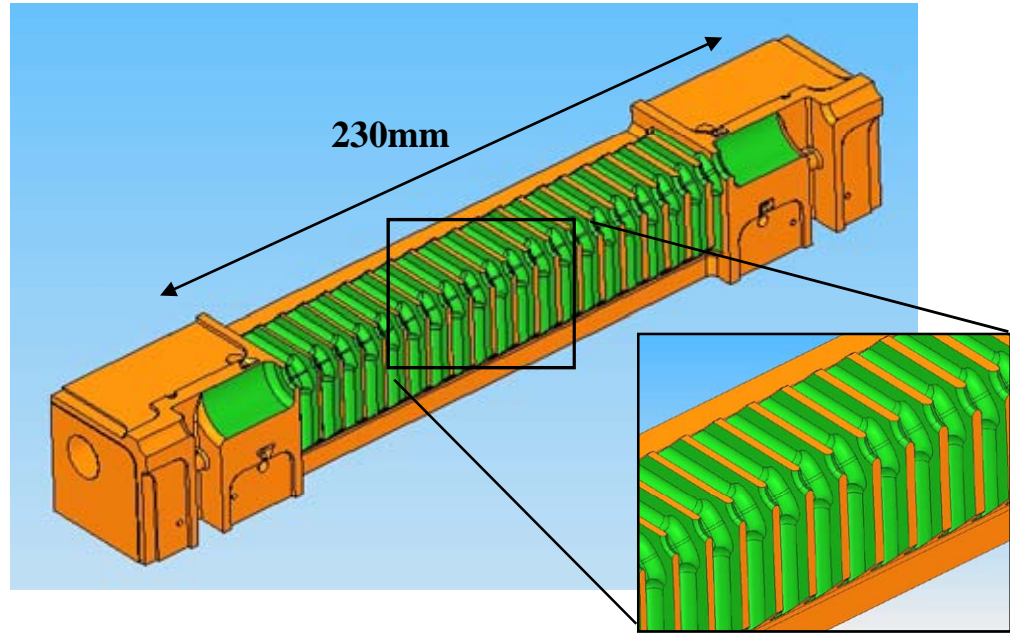
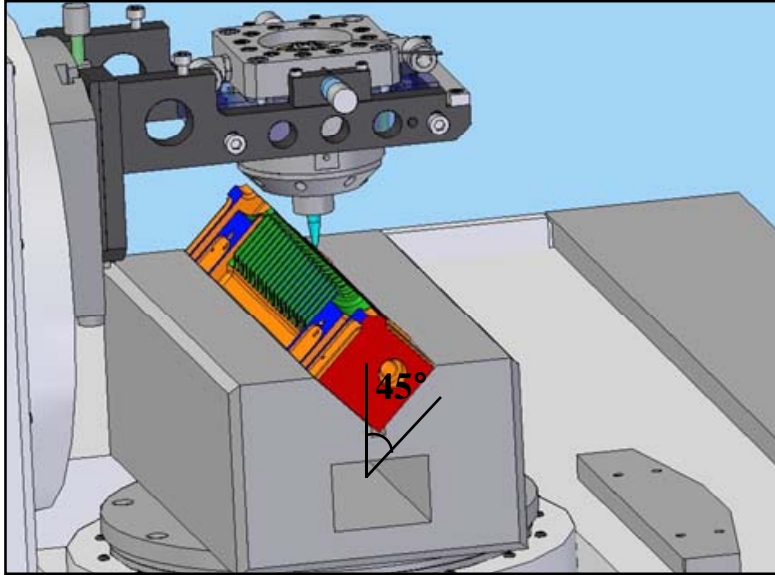
別紙 1 外観

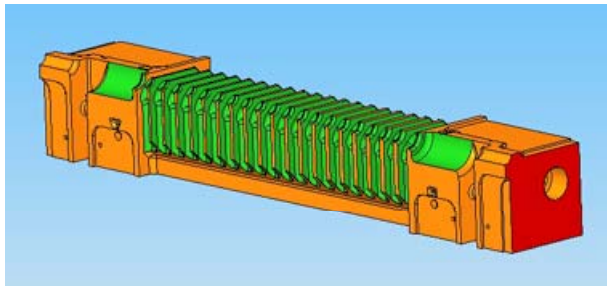
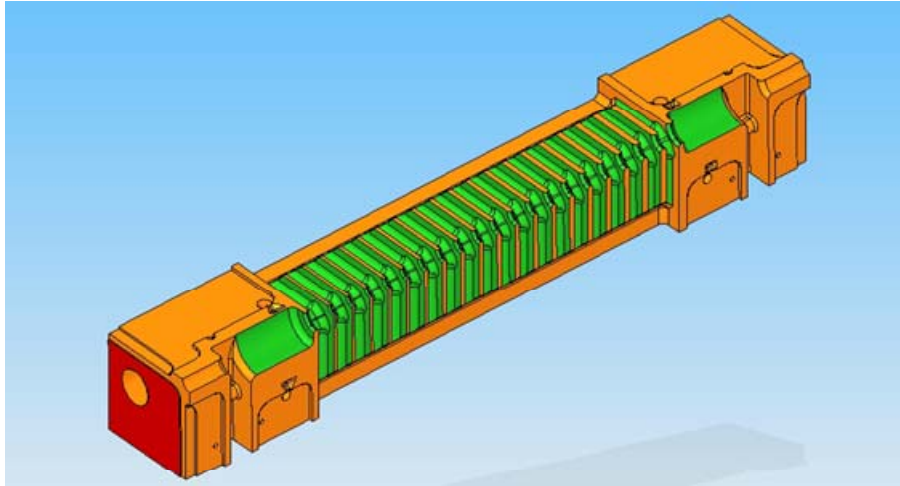
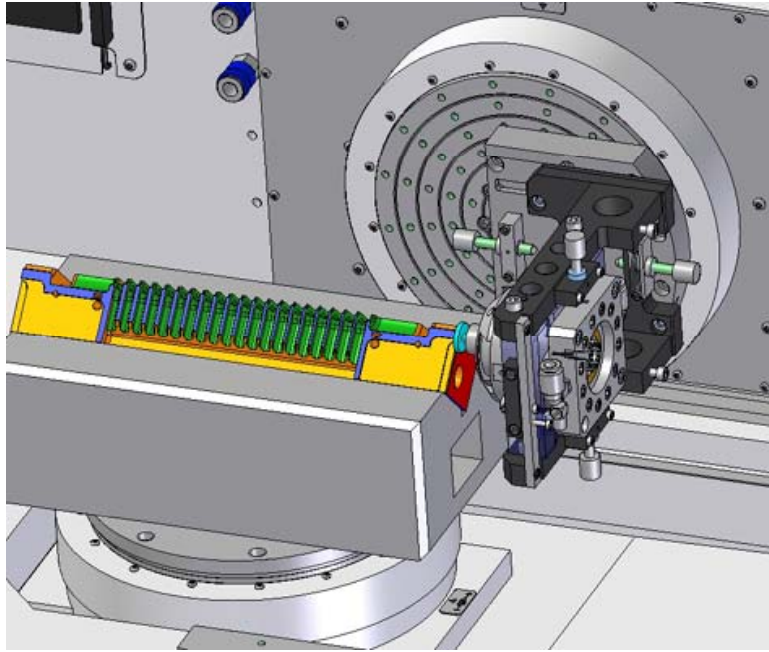


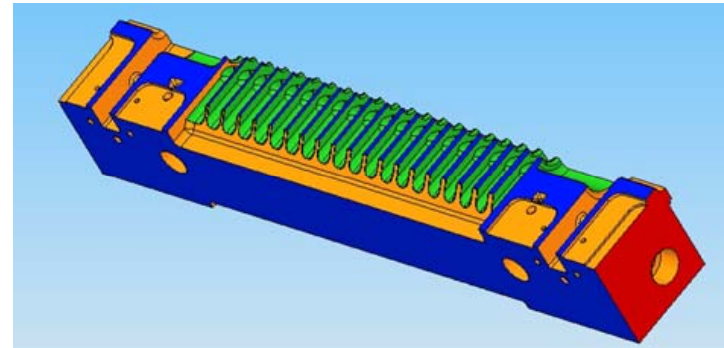
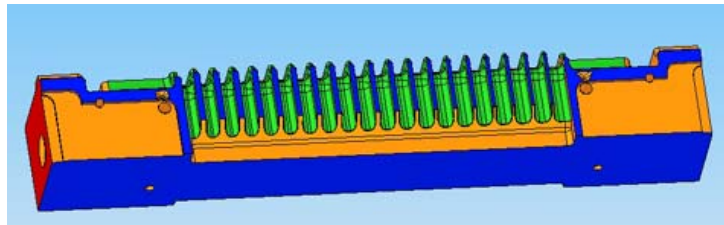
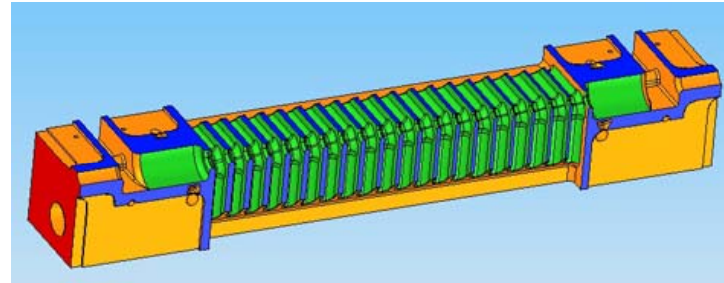
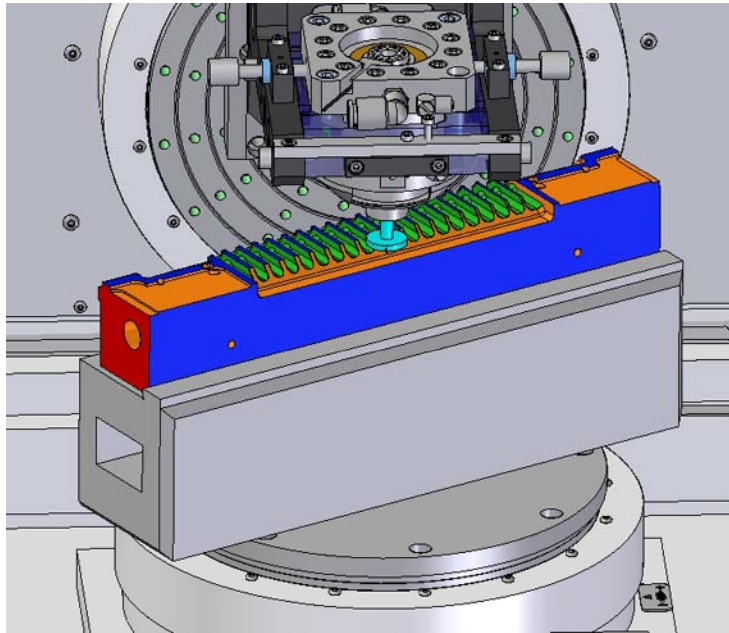
通常切削加工による
実験結果

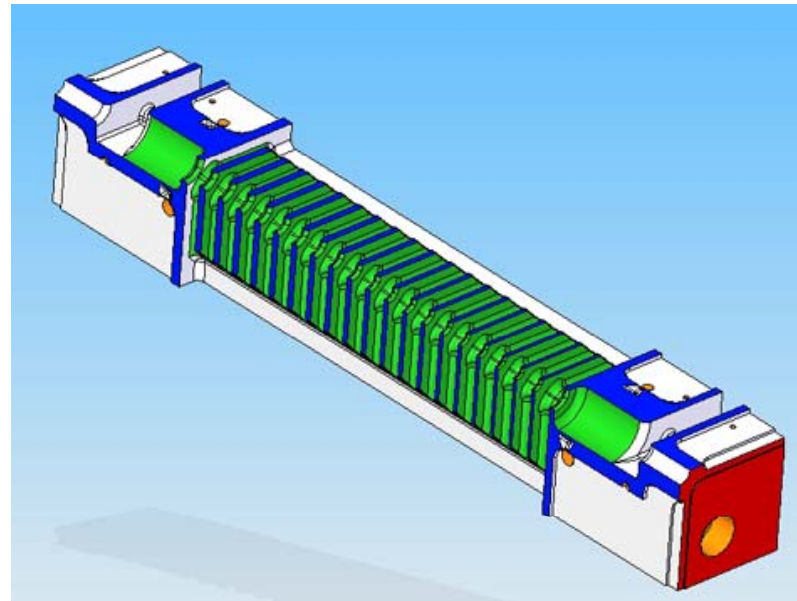
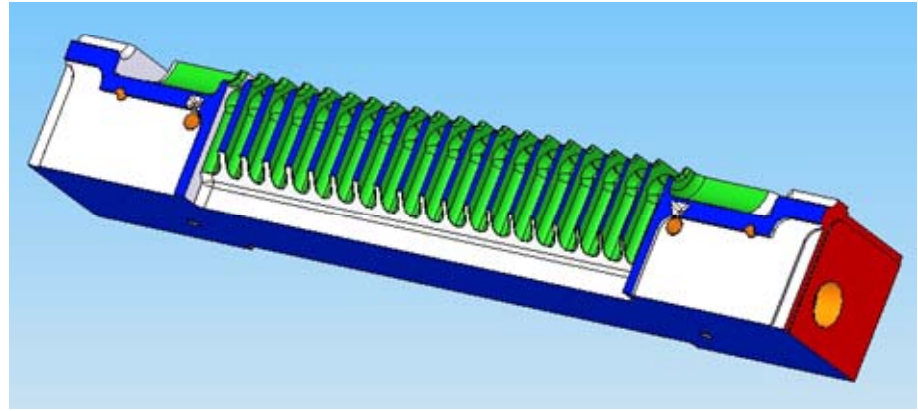
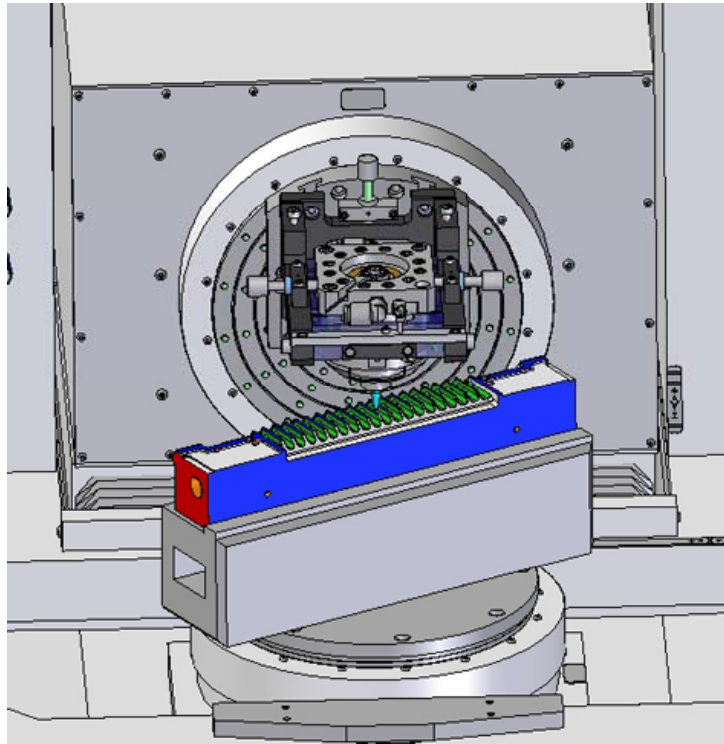
楕円振動切削加工による
実験結果

Quadrant structure fabrication study by FANUC Co.









Summary

- Continually studying surface preparation for
 - Pulse surface heating
 - Break down
- Studying quadrant structure fabrication technologies having low break down rate